

115670  
11-09-92  
115670

OSU-ECE Report NASA 92-02

Phase 2

P.68

Annual Report on

**NONLINEAR STABILITY AND CONTROL STUDY  
OF HIGHLY MANEUVERABLE  
HIGH PERFORMANCE AIRCRAFT**

N92-30922

Unclas

G3/08 0115670

(NASA Grant No. NAG-1-1081)

Date: August 20, 1992

R.R. Mohler, Principal Investigator

Oregon State University  
Department of Electrical and Computer Engineering  
Corvallis, Oregon 97331-3211

(503) 737-3470/3617

(NASA-CR-190667) NONLINEAR  
STABILITY AND CONTROL STUDY OF  
HIGHLY MANEUVERABLE HIGH  
PERFORMANCE AIRCRAFT, PHASE 2  
ANNUAL REPORT (Oregon State Univ.)  
20 P

Graduate Research Assistants: S. Cho, C. Koo, R. Zakrzewski  
Undergraduate Participants (NSF Support): D. Aaberg, J. Young  
Visiting Researchers: J. Dory\*, J. Kurek\*\*, A. Yagen\*  
NASA Fellow: D. Collins

\*ADA-Israel Support  
\*\*International Exchange Board

**OSU-ECE Report NASA 92-02**

**Phase 2**

**Annual Report on**

**NONLINEAR STABILITY AND CONTROL STUDY  
OF HIGHLY MANEUVERABLE  
HIGH PERFORMANCE AIRCRAFT**

**(NASA Grant No. NAG-1-1081)**

**Date: August 20, 1992**

**R.R. Mohler, Principal Investigator**

**Oregon State University  
Department of Electrical and Computer Engineering  
Corvallis, Oregon 97331-3211**

**(503) 737-3470/3617**

**Graduate Research Assistants: S. Cho, C. Koo, R. Zakrzewski  
Undergraduate Participants (NSF Support): D. Aaberg, J. Young  
Visiting Researchers: J. Dory<sup>\*</sup>, J. Kurek<sup>\*\*</sup>, A. Yagen<sup>\*</sup>  
NASA Fellow: D. Collins**

---

**\*ADA-Israel Support**

**\*\*International Exchange Board**

# TABLE OF CONTENTS

	<u>Page</u>
1. OVERVIEW .....	1
2. NONLINEAR MAC ALGORITHM STATUS .....	7
3. TIME-OPTIMAL CONTROL .....	10
3.1 Introduction .....	10
3.2 Switching-Time-Variation Method .....	11
3.3 Approximation for Systems Affine in Control .....	14
3.4 Computer Implementation .....	15
4. SLIDING-MODE CONTROL AND FEEDBACK LINEARIZATION .....	19
4.1 Sliding-Mode Control .....	22
4.2 Feedback Linearization .....	22
4.3 Continuous Sliding-Mode Control with Feedback Linearization .....	26
4.4 Simulation .....	30
5. OTHER PRELIMINARY STUDIES .....	37
5.1 Bilinear-Based Adaptive Control .....	37
5.2 Neural-Net-Based Control .....	38
6. REFERENCES .....	41

## APPENDICES

- A. List of Project Publications
- B. On Nonlinear Model Algorithm Controller Design
- C. Analysis of Nonlinear Stability Using Robust Stability Analysis for Linear Systems

## 1. OVERVIEW

This research should lead to the development of new nonlinear methodologies for the adaptive control and stability analysis of high angle-of-attack aircraft such as the F18 (HARV). The present progress report reviews project research over the second year.

The emphasis has been on nonlinear adaptive control, but associated model development, system identification, stability analysis and simulation is performed in some detail as well. Table 1 summarizes various models under investigation for different purposes.

Models and simulations for the longitudinal dynamics have been developed for all types except 7 in Table 1. A very preliminary analysis has been made on type 6 (neural net models) for adaptive control thus far. It has been shown that dynamic accuracy roughly increases with ascending order of model type from 1 to 7, except that perhaps 3 (Volterra series) and 6 (neural nets) should be interchanged. However, such comparisons depend on how the models are utilized. For example, the neural-net model and subsequent control seems to be more accurate than 1 to 5 for flight profiles outside a priori data sets. Here, the focus is on adaptive control, generated by model-reference types 1 to 6, of a complex nonlinear aircraft motion represented by 7 (nonlinear ordinary differential equations). Preliminary analyses use a nonlinear second-order approximation [1] which we found useful for changes in angle of attack ( $\alpha$ ) by about  $10^\circ$  or possibly  $20^\circ$ . A fifth-order nonlinear longitudinal model with the traditional stability derivatives generated as functions primarily of  $\alpha$ , for a given altitude and mach number, successfully mimicked F18 flight trajectories [2], and is being utilized for our nonlinear adaptive-control studies at the present time. These models are discussed in the project's first annual report [3]. Simulations and studies reported here refer to the complex (fifth-order) longitudinal model unless otherwise noted.

Briefly, studies completed indicate that nonlinear adaptive control can outperform linear adaptive control for rapid maneuvers with large changes in  $\alpha$ . Figures 1 and 2 compare the transient responses where the desired  $\alpha$  varies from  $5^\circ$  to  $60^\circ$  to  $30^\circ$  and back to  $5^\circ$  all in about 16 sec. Here, the horizontal stabilator is the only control used with an assumed first-order linear actuator with a 1/30 sec

Table 1. Aircraft Models

Type	Purpose	Remarks/Limitations
1. Linear perturbations desired $\alpha$ , M, h*	Local control, check of nonlinear system, application of well developed linear control methodologies  Local stability	Only valid for small maneuvers  Special case of types 2-5
2. Gain scheduled (nonlinear function of $\alpha$ ) from 1	Gain-scheduled adaptive control based on well developed methodologies  Simplified description of complex system  Approximate stability	May have stability problems with small number of reference states and/or large fast maneuvers
3. Volterra series† a) at reference states b) general case	Nonlinear adaptive control via cross-correlation and/or a priori dynamic structure  Stability approximation  Simplified dynamic description of complex system	Non-orthogonal series approximation  Sufficiency of 2 or 3 kernels  Large computation time for adaptation
4. Bilinear system a) continuous b) BARMA  5. Polynomial time series	Nonlinear adaptive control via model reference identification (NLMRAC)  Stability approximation  Simplified dynamic description	Large computation time  Bilinearizing controllers may be more practical than linearizing ones  Polynomial approximation may be more accurate but more time consuming than linear or bilinear approximation
6. Neural network	Potential application to adaptive control	Probably less accurate than 4 or 5 for a given data set but accuracy may be more robust outside the available data set
7. Nonlinear ordinary differential equation model	Accurate approximation to fast large maneuvers for "final" design and simulation  Stability	Neglects flexible modes and other complications
8. Nonlinear partial differential equations model	Allows the treatment of distributed external stresses and local pressures as well as internal stresses and deformations	Computations are time consuming  Overall model complexity  Allows one to treat flutter and distributed control strategies, etc.

\*  $\alpha$  is angle of attack, M mach number, and h altitude

† Wiener series can be used for orthogonal representation

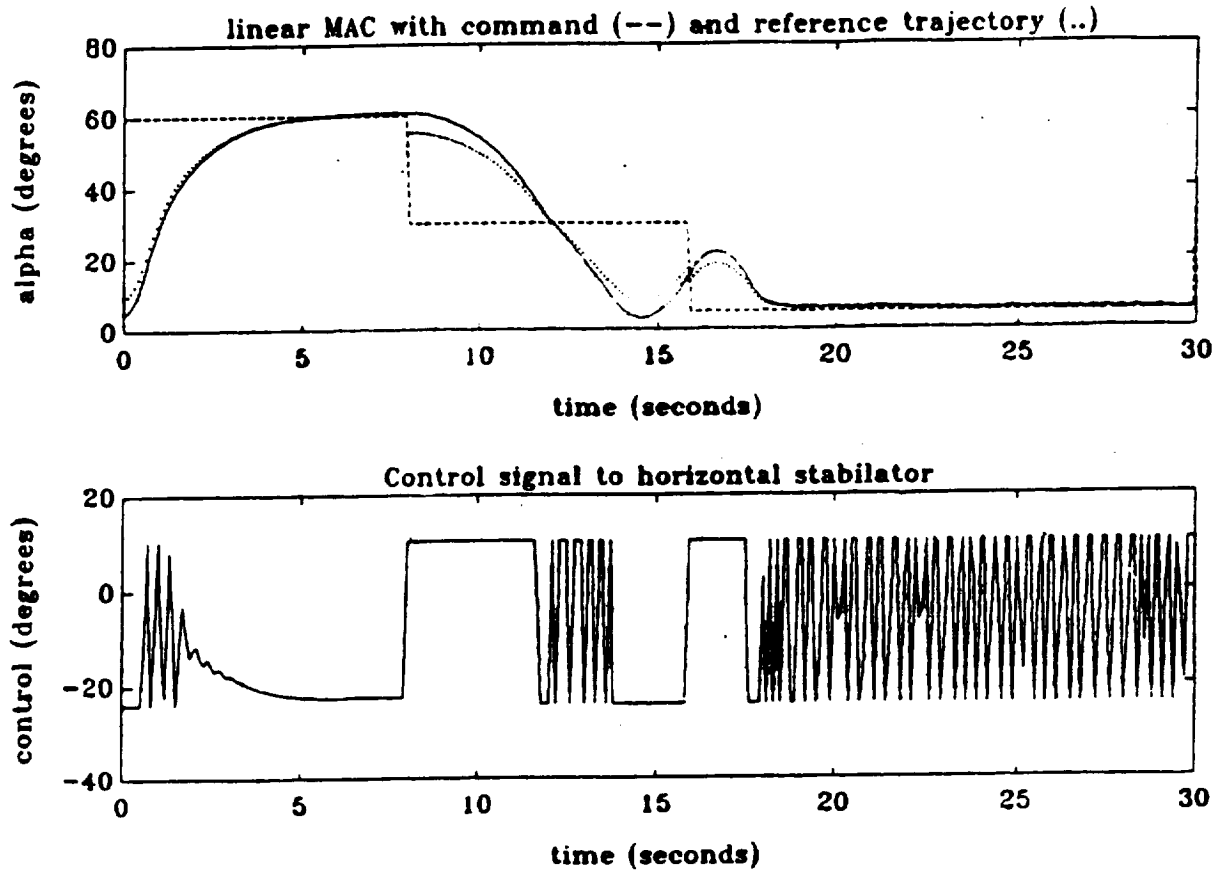


Figure 1. Response for Linear MAC

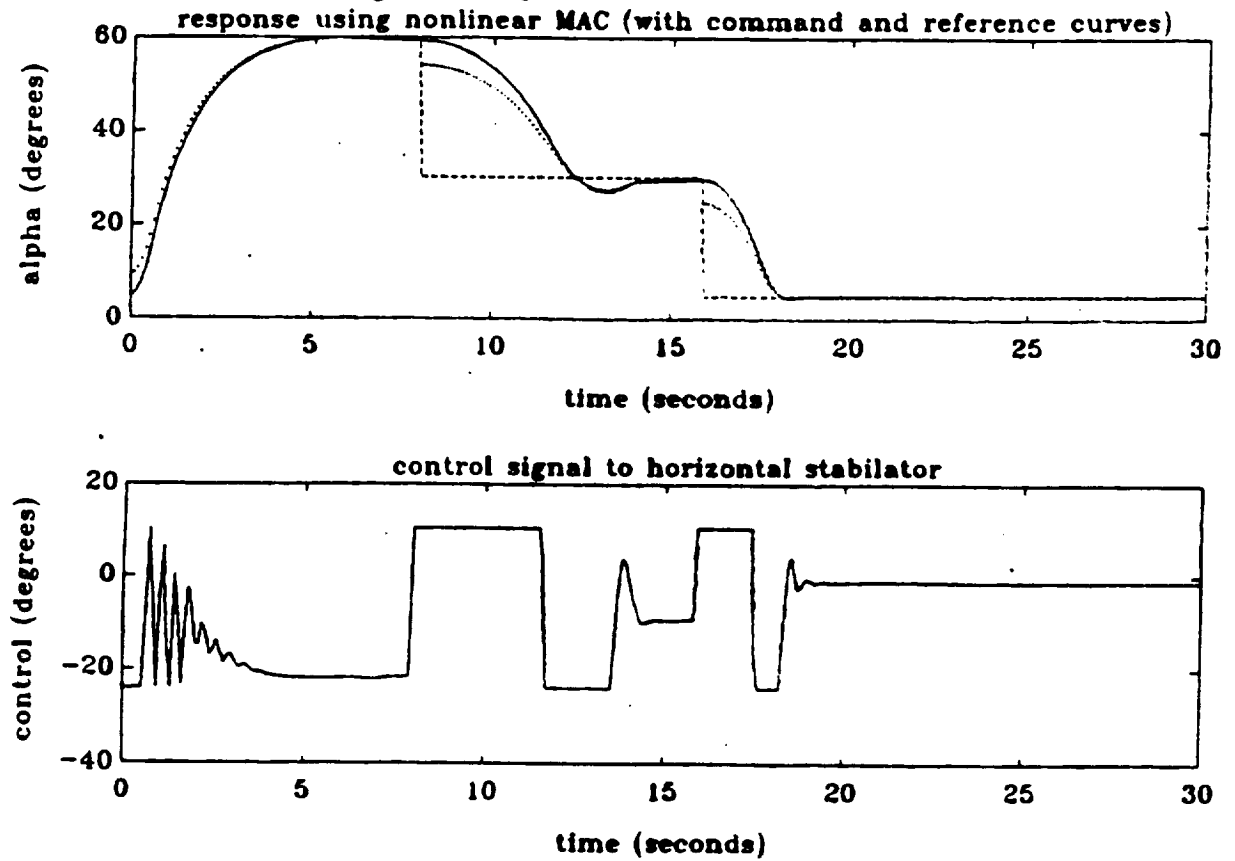


Figure 2. Response for Nonlinear MAC

time constant. Unfortunately, an additional rate constraint significantly reduces the system performance for both the nonlinear and linear adaptive control as shown in Figures 3 to 5 and analyzed in the next section. Such lack of controllability can be improved, of course, by introducing thrust vectoring as used in [2]. Appropriate thrust-vector control to supplement the traditional pitch-motion stabilizers is underway for the nonlinear adaptive controllers, and preliminary results are encouraging.

A preliminary analysis of time-optimal control of  $\alpha$  is studied in Section 3. Here, a new algorithm is derived from the switching-time variational method [4,5] and then applied successfully to the simplified second-order nonlinear model [1]. The method has been adapted to the more complex nonlinear fifth-order model and new simulations are in progress. This study should provide a "yard stick" by which to evaluate controller performance as well as provide a base for more effective controller designs. For example, it might be used in conjunction with a neural-net generated approximately, time-optimal feedback controller as introduced in Section 5.2. As a byproduct of this analysis the complicated Jacobian of the longitudinal dynamics will be computed as a function of  $\alpha$  and other variables. While it is used here to compute bang-bang controller switching times, it should have other uses for approximate dynamic-system identification beyond the usual time-invariant linearized models at trim states.

Nonlinear PIF (proportional plus integral plus filter) control as a generalization of the linear PIF control is being studied. The linear PIF controller developed by Ostroff at NASA-LaRC has shown remarkable success in simulations as demonstrated in [4] and by more recent simulations and flight tests at NASA-LaRC on HARV. The first nonlinear PIF controller which we are investigating involves a bilinear (linear with parametric control) model reference for basic control philosophy. For example, the PIF model reference may be established from a simplified/approximated time-optimal solution. Then a bilinearization of the complex nonlinear aircraft about say an approximate time-optimal trajectory can be used to generate the PIF control by possibly an optimal control such as with a quadratic performance index. This is introduced briefly in Section 5.1.

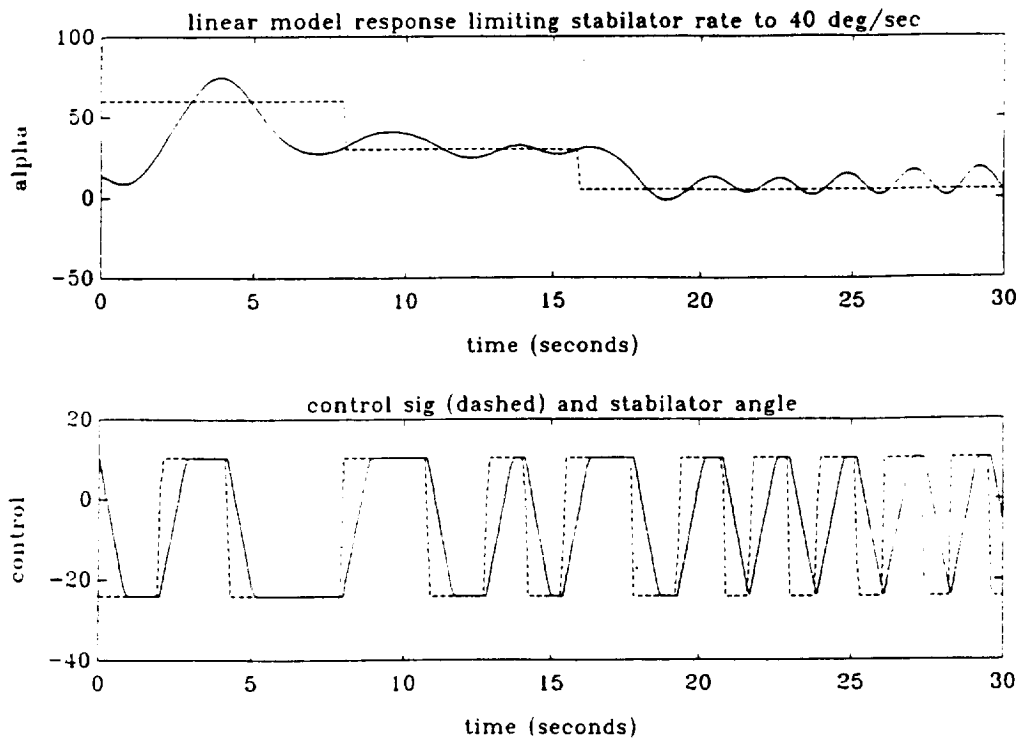


Figure 3. Response of Linear MAC with Stabilator Limit of 40° per Second

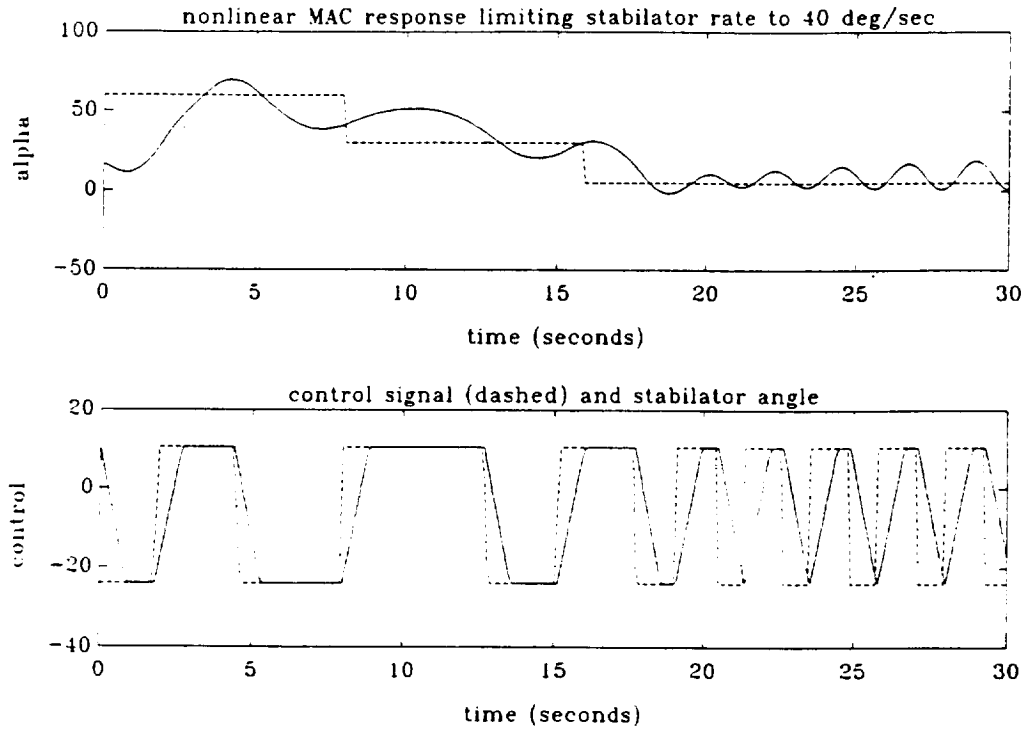


Figure 4. Response of Nonlinear MAC with Stabilator Limit of 40° per Second

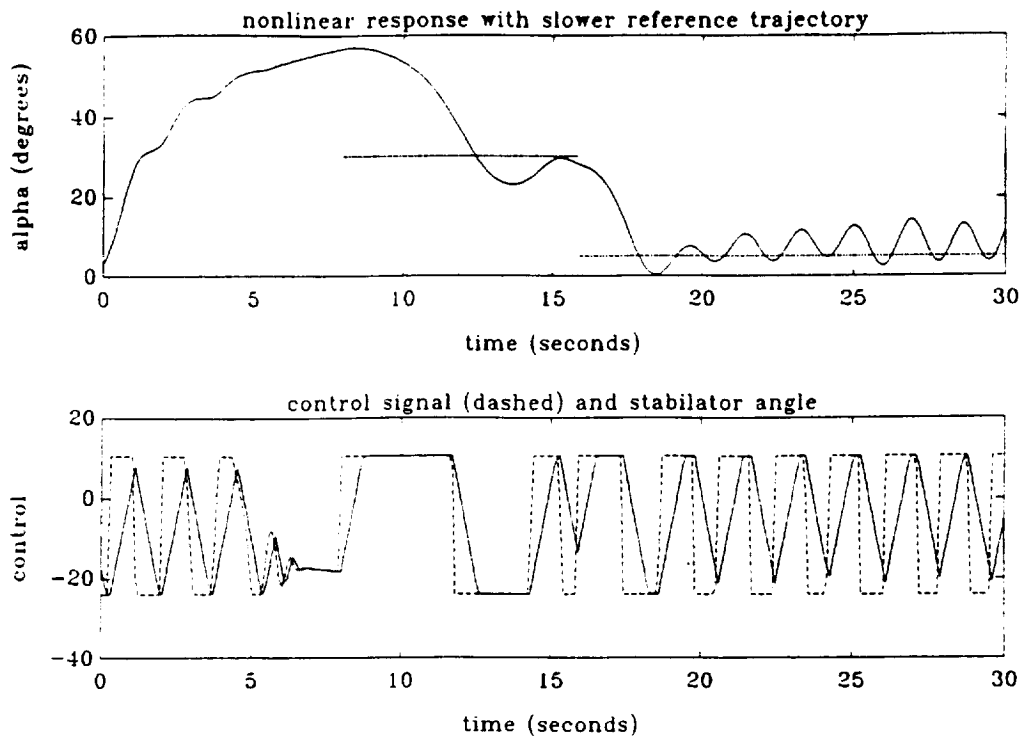


Figure 5. Response for Nonlinear MAC with Stabilator Limit of  $40^\circ$  per Second and Slower Reference Trajectory

Feedback linearization and variable-structure or sliding-mode control also are being investigated in this project. Both generally have major robustness problems for complex nonlinear dynamics with major unknown components and control constraints such as HARV due to aerodynamic stability-derivative uncertainty and available actuators. However, they might be useful as a foundation for more complex nonlinear controller design synthesis. Also, they can be useful to provide benchmarks of performance for comparison with time-optimal controls and other nonlinear controls studied here. At the other extreme, a comparison with robust linear controllers will also be made.

A cursory analysis (presented in Section 4) suggests that robust linearizing controllers (as well as robust linear controllers) of sufficient complexity may very well stabilize the longitudinal HARV motion for even large deviations from trim flight, but there most likely would be considerable reduction in maneuverability along with transient overshoot — the two of which exhibit some tradeoff. It should be

noted here that linear adaptive control really involves nonlinear feedback which can be thought of as a bilinear system (linear system with parametric control). In conjunction with linear model-reference adaptive control, the nonlinear feedback essentially becomes a feedback-linearization process, and again may suffer the corresponding drawbacks in practice.

Also, it should be noted that ideally, at least, the sliding-mode control (with probable chatter) can conveniently be implemented to accommodate state constraints (as an alternative to excessive overshoot) such as can arise from the time-optimal case. But, again, its feasibility with the physical actuator's rate and accelerating constraints needs to be studied further.

Finally, linear stability arguments are developed in Appendix C which tend to at least an approximation of the admissible range of model parameters as applied to the nonlinear second-order approximation [1].

## 2. NONLINEAR MAC ALGORITHM STATUS

Model algorithmic control (MAC), described in [3], starts with

$$\alpha_{\text{ref}}(k+1) = \alpha_{\text{mod}}(k+1) + (\alpha(k) - \alpha_{\text{mod}}(k)) \quad (1)$$

where

$$\alpha_{\text{mod}}(k+1) = p_a^T \phi(k) \quad (2)$$

$$\phi(k) = [\alpha, \alpha^2, \alpha^3, q, q\alpha, qa^2, q\alpha^3, u, u\alpha, u\alpha^2, u\alpha^3, 1]^T(k) \quad (3)$$

As the control at the moment  $k$  must be already computed at moment  $k$  the values of  $\alpha(k)$  and  $q(k)$  are not available for its computation so their estimates must be used instead. The correction term is taken to be the prediction error from the moment  $k-1$  and the equation becomes

$$\alpha_{\text{ref}}(k+1) = \hat{\alpha}_{\text{mod}}(k+1) + (\alpha(k-1) - \alpha_{\text{mod}}(k-1)) \quad (4)$$

with

$$\begin{aligned}\hat{\alpha}_{\text{mod}}(k+1) &= p_{\alpha}^T \hat{\phi}(k) \\ \hat{\phi}(k) &= [\hat{\alpha}, \hat{\alpha}^2, \hat{\alpha}^3, q, q\hat{\alpha}, q\hat{\alpha}^2, q\hat{\alpha}^3, u, u\hat{\alpha}, u\hat{\alpha}^2, u\hat{\alpha}^3, 1]^T(k) \\ \hat{\alpha}(k) &= p_{\alpha}^T \phi(k-1) + (\alpha(k-1) - \alpha_{\text{mod}}(k-1)) \\ \hat{q}(k) &= p_q^T \phi(k-1) + (q(k-1) - q_{\text{mod}}(k-1))\end{aligned}$$

The controller is assumed to know the values of angle of attack and of pitch rate at the moment  $k-1$ . Then it estimates their current values  $\alpha(k)$  and  $q(k)$  taking into consideration previous prediction errors, and based on them it calculates the control required to achieve  $\alpha_{\text{ref}}$  at the moment  $k+1$ . The value of control is found as:

$$u(k) = \frac{\tilde{\alpha}_r - p_{1\alpha}\hat{\alpha} - p_{2\alpha}\hat{\alpha}^2 - p_{3\alpha}\hat{\alpha}^3 - p_{4\alpha}\hat{q} - p_{5\alpha}\hat{q}\hat{\alpha} - p_{6\alpha}\hat{q}\hat{\alpha}^2 - p_{7\alpha}\hat{q}\hat{\alpha}^3 - p_{12\alpha}}{p_{8\alpha} + p_{9\alpha}\hat{\alpha} + p_{10\alpha}\hat{\alpha}^2 + p_{11\alpha}\hat{\alpha}^3} \quad (5)$$

where

$$\tilde{\alpha}_r = \alpha_{\text{ref}}(k+1) - (\alpha(k-1) - \alpha_{\text{mod}}(k-1)) \quad (6)$$

and  $\hat{\alpha} = \hat{\alpha}(k)$ ,  $\hat{q} = \hat{q}(k)$  as described above.

This algorithm was made to be adaptive, or self-tuning, by incorporating on-line identification of the parameters. A recursive least squares (RLS) algorithm was implemented in the form taken from

$$p(k) = \frac{Q(k-2) \phi(k-1)}{\lambda(k-1) + \phi(k-1)^T Q(k-2) \phi(k-1)} \quad (7)$$

$$Q(k-1) = \frac{1}{\lambda(k-1)} \left[ Q(k-2) - \frac{Q(k-2) \phi(k-1) \phi(k-1)^T Q(k-2)}{\lambda(k-1) + \phi(k-1)^T Q(k-2) \phi(k-1)} \right] \quad (8)$$

$$e(k-1) = y(k) - p^T \phi(k-1) \quad (9)$$

where  $y$  may denote  $\alpha$  or  $q$  and  $p$  may stand for  $p_\alpha$  or  $p_q$ , respectively. The forgetting factor  $\lambda$  was introduced to enable the algorithm to change the estimates of parameters with the change of operating conditions. To avoid the unlimited growth of covariance matrix  $Q$  at the steady state when the input is not persistently exciting, the variable forgetting factor policy was implemented:

$$\lambda(k) = 1 - \epsilon \frac{e(k)^2}{\bar{e}(k)^2} \quad (10)$$

where  $e(k)$  is the current prediction error,  $\bar{e}(k)$  is the average prediction error from last 10 samples, and  $\epsilon$  is equal to 0.01. As an additional precaution, the trace of the covariance matrix  $Q$  was monitored and  $Q$  was reset to diagonal matrix whenever the threshold value was exceeded.

To further damp the response, the controller is designed to minimize the one step ahead cost function:

$$J = (y_{\text{mod}}(k+1) - \tilde{y}_r(k))^2 + \rho(u(k) - u(k-1))^2 \quad (11)$$

with  $y_{\text{mod}}$ ,  $\tilde{y}_r$  as before. Minimization of (11) with respect to  $u(k)$  yields

$$u(k) = \frac{(\tilde{y}_r - a)b + \rho u(k-1)}{b^2 + \rho} \quad (12)$$

where

$$a = p_{1\alpha}\alpha + p_{2\alpha}\alpha^2 + p_{3\alpha}\alpha^3 + p_{4\alpha}q + p_{5\alpha}q\alpha + p_{6\alpha}q\alpha^2 + p_{7\alpha}q\alpha^3 + p_{12\alpha}$$

$$b = p_{8\alpha} + p_{9\alpha}\alpha + p_{10\alpha}\alpha^2 + p_{11\alpha}\alpha^3$$

Obviously, for  $\rho = 0$  (12) reduces to (5) while for  $\rho = \infty$  we have  $u(k) = u(k-1) = \text{const.}$

This controller is used in Figures 2, 4, and 5 with only the linear portion of  $a, b$  used in Figures 1 and 3. The algorithm will be generalized to include thrust vector control and variable-horizon cost.

### 3. TIME-OPTIMAL CONTROL

#### 3.1 Introduction

Various control strategies have been developed by the team and to find their merits it seems useful to have an idea of what are the best output and state trajectories theoretically possible, given the existing constraints on the control variables. For substantially nonlinear systems the problem of synthesis of the optimal feedback control law is usually untractable. On the other hand, there exist numerical techniques that allow us to calculate "open loop controls" - i.e., the specific control signals necessary to achieve the minimum performance index. Aware of the difficulties connected with the controller synthesis problem we do not seek its exact solution; at this time, we merely want to find the limit for the performance of a controller assuming perfect knowledge of plant dynamics and absence of any unforeseen disturbances.

This report is concerned with the problem of time-optimal control in which we are interested in transferring the system's state from an initial value to some prescribed terminal set in minimal time. In the aircraft problem this might mean changing the flight's pitch angle, path angle, or angle of attack from an initial equilibrium value to some other terminal value, preferably also with all other states moving to the equilibrium. The control value (stabilator or elevator angle) is naturally bounded from below and from above. For some systems it turns out that in case of such simple cube-type constraints on control variables, the time-optimal control is of bang-bang type. However, for quite a large class of systems that are affine in control, we may approximate any measurable control signal with a bang-bang signal with arbitrary accuracy in the sense that corresponding state trajectories are arbitrary close to each other in  $L^1$  metric. Hence, also time-optimal control, if it exists, may be approximated by a bang-bang control, even if it contains singular arcs. Therefore, the approach presented here is to find the bang-bang control that will minimize the transition time. The computational algorithm used here is the switching-time-variation method developed in [4,5]. Since the algorithm gives as an output a control signal with finite number of switchings, it is tacitly assumed that with large enough finite number of switchings, we are able to achieve good enough approximation of optimal control. This, unfortunately, does not follow from

the theory I am aware of, since the above mentioned approximation result holds only for bang-bang signals with possibly infinite or even uncountable number of switchings. This delicate question is left aside for the time being to be clarified later. Another point worth indicating here is that resulting control, in an attempt to approximate a continuous "singular" control, may have inter-switching times very small, thus precluding any practicality of the approximation. This, however, is of no concern to us since, as mentioned before, we are interested only in finding the best possible output, or state, trajectories - not the actual control signals corresponding to them at this time.

A computer program has been developed for numerical solution of the problem. The program, due to its modular construction, easily allows various plant models to be plugged into it. The switching-time-variation method is used in it for fixed terminal time with the quality function being the weighted distance of the target set. Then the smallest such time is found that allows it to hit the target exactly, and finally the optimal number of switchings is iteratively found that gives minimal transition time.

In what follows the switching-time-variation method is briefly characterized in Section 3.2. Section 3.3 discusses briefly the approximation theorem for bang-bang controls in systems affine in control. The computer implementation of the algorithm is discussed in Section 3.4. Section 3.5 contains the test results of the program for a second-order model of longitudinal dynamics of an aircraft. The concluding remarks discuss the possibilities of application of the computer package to solutions of more complex and problems more close to reality.

## 3.2 Switching-Time-Variation Method

The switching-time-variation method used here was taken from [4], and the original thesis [5] was also consulted for the details. The method is designed for the computation of optimal control in the class of bang-bang control signals with finite number of switchings. The quality criterion is assumed to be

$$J = \int_{t_0}^{t_f} (f_0(x) + g_0(x) u(t)) dt \quad (13)$$

for the system of the form

$$\frac{dx}{dt} = f(x) + g(x)u(t) \quad (14)$$

where  $x \in \mathbf{R}^n$ ,  $u \in \mathbf{R}^1$ ,  $t \in [t_0, t_f]$ . To ensure the existence and uniqueness of solutions of (14),  $f$  and  $g$  are assumed to be continuously differentiable with respect to  $x$ . The control values are constrained by

$$-1 \leq u(t) \leq 1 \quad (15)$$

Of course, any control constraints of the cube-like type  $u_{\min} \leq u(t) \leq u_{\max}$  may be transformed to form (15) for system affine in control. The control objective is to minimize the quality criterion (13) for given initial state  $x_0$  with possible penalty term connected with final state already included in  $f_0$  and  $g_0$  by standard transformations, assuming that admissible controls are bang-bang with finite number of switchings. The version of the algorithm described in [4] was developed for systems with scalar controls and the computer program described here is also designed for this special case. However, it is not of any particular difficulty to generalize the algorithm to the case of  $u \in \mathbf{R}^m$ . If the need arises, the computer program may also be modified to accommodate this possibility. Here the scalar version will be presented because of its notational simplicity.

The method is an iterative one - in each step the gradient of the quality criterion with respect to switching times is computed. The switching vector is defined as:

$$\tau = (\tau_1, \dots, \tau_N) \quad (16)$$

where  $N$  is the number of switchings, with constraints:

$$t_0 \leq \tau_1 \leq \dots \leq \tau_N \leq t_f \quad (17)$$

The control value on the interval  $[\tau_i, \tau_{i+1})$  is then equal  $(-1)^i$ . The augmented system is defined as:

$$\frac{d\bar{x}}{dt} = \bar{f}(\bar{x}) + \bar{g}(\bar{x})u(t) \quad (18)$$

where  $\tilde{f}^T = (f_0, f^T)$ ,  $\tilde{t}^T = (g_0, g^T)$ ,  $\tilde{x}_0^T = (0, x_0^T)$ , and the adjoint system equation is

$$\frac{d\lambda}{dt} = - \left[ \frac{\partial \tilde{f}}{\partial \tilde{x}}(t) + \frac{\partial \tilde{g}}{\partial \tilde{x}}(t) u(t) \right]^T \lambda \quad (19)$$

with terminal conditions  $\lambda_i(t_f) = (\partial J / \partial \tilde{x}_i)(t_f)$ . Then the gradient of the quality criterion with respect to the switching vector may be calculated by means of the formula

$$\frac{\partial J}{\partial \tau_i} = (-1)^{i-1} \phi(\tau_i) \quad (20)$$

with function  $\phi$  defined by

$$\phi(t) = 2 \langle \tilde{g}(\tilde{x}(t)), \lambda \rangle \quad (21)$$

with gradient calculated the method consists of iterative descent steps

$$\tau_i(k+1) = \tau_i(k) + k_i \frac{\partial J}{\partial \tau_i} \quad (22)$$

where  $k_i$  are such that constraints (17) are satisfied and sufficiently small to ensure that  $J(k+1) < J(k)$ . The algorithm is terminated if either the gradient is zero or no feasible (i.e., descent) step may be executed.

On top of the algorithm of finding the optimal switchings with their number given there is an outer loop modifying this number. If the optimal control results in a constraints  $\tau_i \leq \tau_{i+1}$  active than the switchings  $i$  and  $i+1$  should be removed. On the other hand, if there are two zeros of  $\phi(t)$  not coinciding with any of the switching times than two switchings should be added between these zeros. After the modifications of the dimensionality of the switching vector the inner loop of optimization is again performed and the process is terminated when no more changes of the number of switches are necessary.

It is worth noticing that the above algorithm of finding the optimal bang-bang control may be also generalized for broader class of systems  $dx/dt = f(x(t), u(t))$ . The main difference would be the formula for function  $\phi(t_0)$  which would become

$$\phi(t) = \left\langle \left( f(x(t), u_{\max}) - f(x(t), u_{\min}) \right), \lambda \right\rangle \quad (23)$$

Of course, the technical assumptions ensuring the existence of solutions should be satisfied.

### 3.3 Approximation for Systems Affine in Control

The algorithm described above calculates the optimal control within the class of bang-bang control. However, for systems affine in control a result is available stating that we may approximate an arbitrary admissible control with a bang-bang control such that corresponding trajectories are arbitrary close.

The theorem, stated and proven in [6], assumes that we have a system of the form (14) with constraints (15). Functions  $f$  and  $g$  are continuously differentiable, and a Lipschitz type condition  $\langle f(x) + g(x)u, x \rangle \leq K(1 + \|x\|^2)$  preventing finite escape-time is also assumed to be satisfied for all  $x$  in the region of interest. Then an arbitrary measurable control signal  $u(t)$ ,  $t \in [t_0, t_f]$  satisfying (15) is considered with corresponding state trajectory  $x(t)$ . Then the theorem states that given any  $\epsilon > 0$  is always possible to find a bang-bang control  $u^*(t)$  satisfying  $|u^*(t)| \leq 1$ , such that the corresponding state trajectory  $x^*(t)$  approximates  $x(t)$  uniformly on  $[t_0, t_f]$  with accuracy less than  $\epsilon$ , i.e.,  $|x(t) - x^*(t)| \leq \epsilon$  for all  $t \in [t_0, t_f]$ .

Although the theorem stated above considers a bang-bang control with not necessarily finite or even countable number of switchings, it gives some justification to using the switching-time-variation method for systems with singular optimal controls. Intuitively for reasonably smooth systems there should be some kind of continuity enabling in turn approximating the bang-bang control  $u^*$  with a sequence of bang-bang signals  $u$  with finite number of switchings. However, we are not aware of any such result, and in monograph [7] from 1990 the aforementioned result is cited after [6] as the only one available. It still seems feasible to come up with some, maybe more restrictive, assumptions which would justify using finite number of switchings.

### 3.4 Computer Implementation

The algorithm discussed in Section 3.2 was implemented as a quite general software package. It finds the time-optimal control for the case when the terminal set is a single point  $y$ . The time-optimal problem with fixed terminal set is replaced with a sequence of fixed time and free terminal state problems with quality index

$$J = \sum \rho_i (x_i(t_f) - y_i)^2 \quad (24)$$

Switching-time-variation method is used to solve this problem, and the desired final time is decreased if the resulting quality is zero or is increased in the opposite case. This iteration is repeated until we get to the limit time  $t_f^*$  below which the quality is always positive, i.e., it is not possible to find a bang-bang control transferring the system from  $x_0$  to  $y$ .

The optimization method described in Section 3.2 was modified somewhat in details of the gradient minimization routine. Instead of performing single step in the direction, a directional search is performed with constrained step size. A combination of two-point gradient parabolic approximation and three-point non-gradient parabolic approximation is used to find the minimum in the direction. The generation of the descent direction is also somewhat different. First, if any of the constraints (15) are active and the gradient points outside the feasible region, the gradient is projected on the proper constraining hyperplane. The special structure of constraints causes the projection to consist solely of putting the appropriate coordinates of the gradient to zero. Then the direction is tangent to the constraining hyperplane, and we get an optimization problem of reduced dimensionality. This problem is solved using a conjugate gradient method in the version proposed in [6]. The conjugate gradient is restarted not only every  $N$  iterations, where  $N$  is the current dimensionality of the problem, but also whenever the set of active constraints changes - i.e., when the algorithm hits or leaves a constraining hyperplane. The termination of the procedure occurs when the projected gradient is zero - i.e., no feasible descent step is possible, or equivalently when the dimension of the current optimization hyperplane becomes zero.

The calculation of the quality criterion and of its gradient involves numerical integration of Eqs. (18) and (19). This is done using a fourth-order Runge-Kutta integration method. To integrate the adjoint equation (19) the whole state trajectory resulting from integrating (18) must be stored, but for calculation only a small number of points from the costate trajectory is needed.

The program is written in the fashion enabling easy substitutions of different plant models and different optimization tasks. To use another model one has simply to provide the routines calculating the right-hand sides of Eqs. (18) and (19). The problem is defined in a straightforward fashion by setting the values of initial state, terminal state, initial estimate of the final time, etc., in the main routine. The whole program is written in C programming language, and although compiled and run on an IBM PC, it may be easily ported to any machine with C language compiler. The only difficulty that may occur with more complex systems is the rather severe storage requirements - whole state trajectory has to be stored with sufficiently small discretization step in order to calculate the gradient. And, of course, there will always be the problem with the speed of calculations for higher dimensional systems.

The program described above was tested on a model previously used (in our NASA project), i.e., a simplified longitudinal aircraft model of second order described in [6]. For the aircraft model the problem solved was to increase or decrease the value of angle of attack between trim states. The control signal, the elevator angle, was assumed to be between 0 and -20 degrees. A series of maneuvers were simulated and reported in [8]. A typical case is shown in Figures 6a and b for maneuvers between  $0^\circ$  to  $20^\circ$  and  $20^\circ$  to  $0^\circ$ . It may be observed that the time-optimal control has only one switch for the simplified nonlinear model, but the trajectory for  $\alpha$  had a substantial overshoot, and consisted of an almost linear first portion with high slope before the switch and of slowly decreasing second portion.

The computer program presented here is suitable for calculating the time-optimal controls for arbitrary finite-dimensional systems which are affine in control. The simulation results discussed here have mainly testing value showing that the program is in operation. The next step, which is nearing completion, uses the program on more complex models such as a fifth-order longitudinal-aircraft model

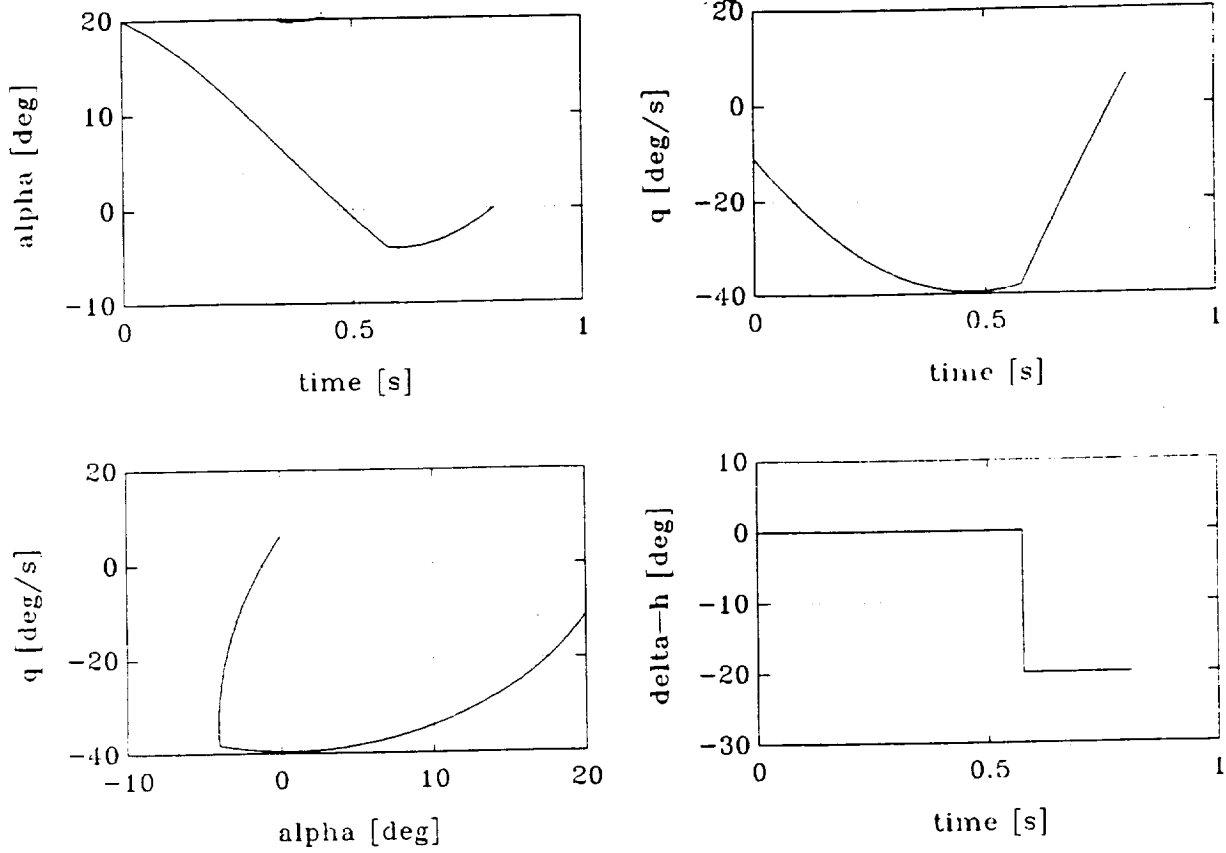


Figure 6. Maneuver C' (from 20 to 0 degrees) .

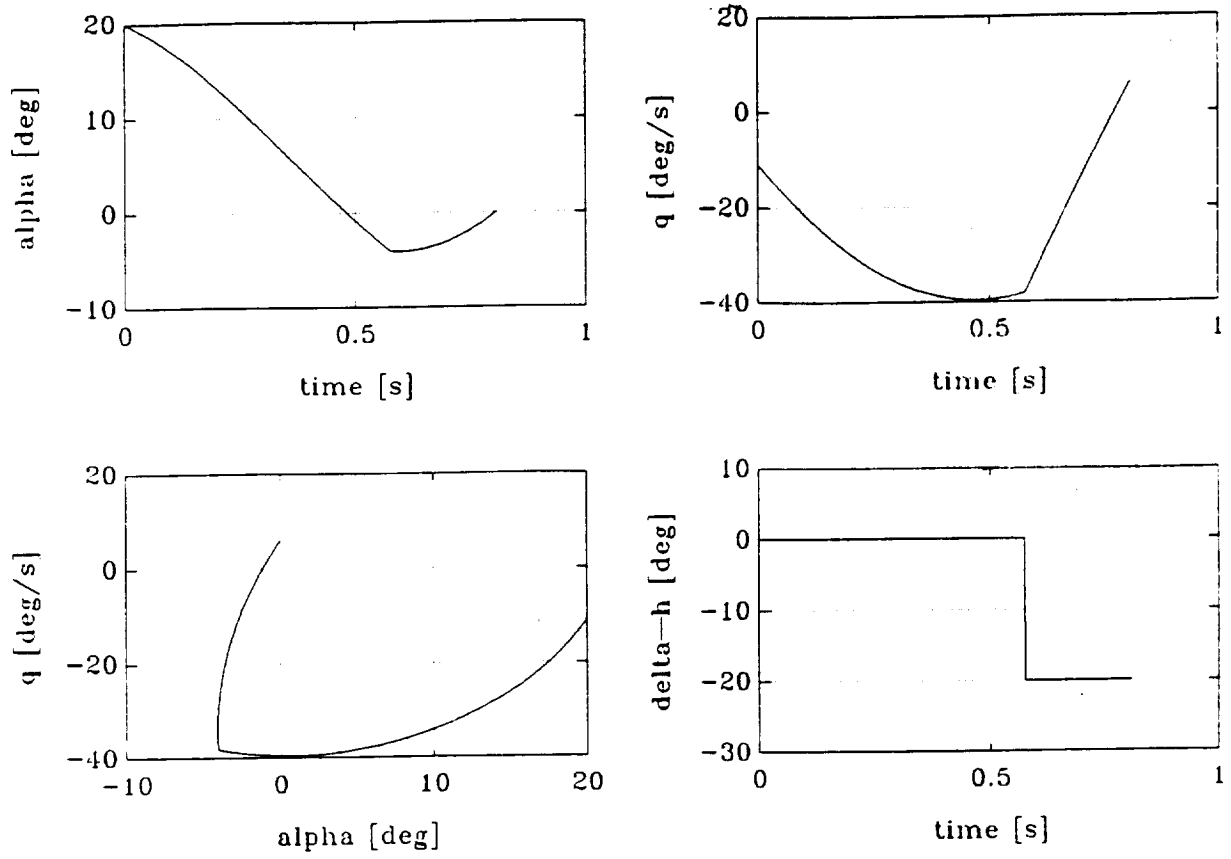


Figure 6b. Alpha Maneuver from 20 to 0 degrees

with a linear actuator and affine in control. The resulting time-optimal trajectories for different maneuvers could be used as benchmark tests for other controllers or as reference trajectories for time-series-based, adaptive, PIF, one-step-ahead (or many-steps-ahead) control.

For large variations in pitch and angle of attack of the complex model it is found that numerous switchings are required and it appears that for extreme cases a singular solution exists for the time-optimal control. (Such solutions evolve when extremal trajectories exist with a zero-valued control switching function.) To handle such cases more efficiently and more accurately, a new algorithm was developed which solves the optimal control problem for a sequence of fixed terminal times with quadratic criteria in errors about the desired terminal state.

Figures 7 and 8 show simulated examples of F-18 maneuvers from trim with pitch  $\theta(0) = \alpha(0) = 5^\circ$ , stabilator angle  $\delta(0) = -7^\circ$ , and constant thrust force of 2956 pounds without thrust vectoring and actuator velocity constraints beyond the  $30 \text{ sec}^{-1}$  lag. Figures 7 and 8 show the simulated time-optimal maneuvers from this trim state to  $\theta = 40^\circ$ ,  $\alpha = 30^\circ$ ,  $q = \dot{\theta} = 0$  in about 1.4 sec. and to  $\theta = 80^\circ$ ,  $\alpha = 72^\circ$  in about 1.9 sec. These results are considered to be of a preliminary nature with further system complications (thrust vector control, actuator rate limits, etc.) being incorporated into the analysis.

#### **4. SLIDING-MODE CONTROL AND FEEDBACK LINEARIZATION**

Sliding-mode control and feedback linearization can be used in an integrated manner sometimes to control effectively nonlinear dynamical plants. Unfortunately, both can suffer considerable performance deterioration in the presence of dynamic uncertainty and control constraints for some physical applications [3,9]. These aspects need further study with the material presented here only a start.

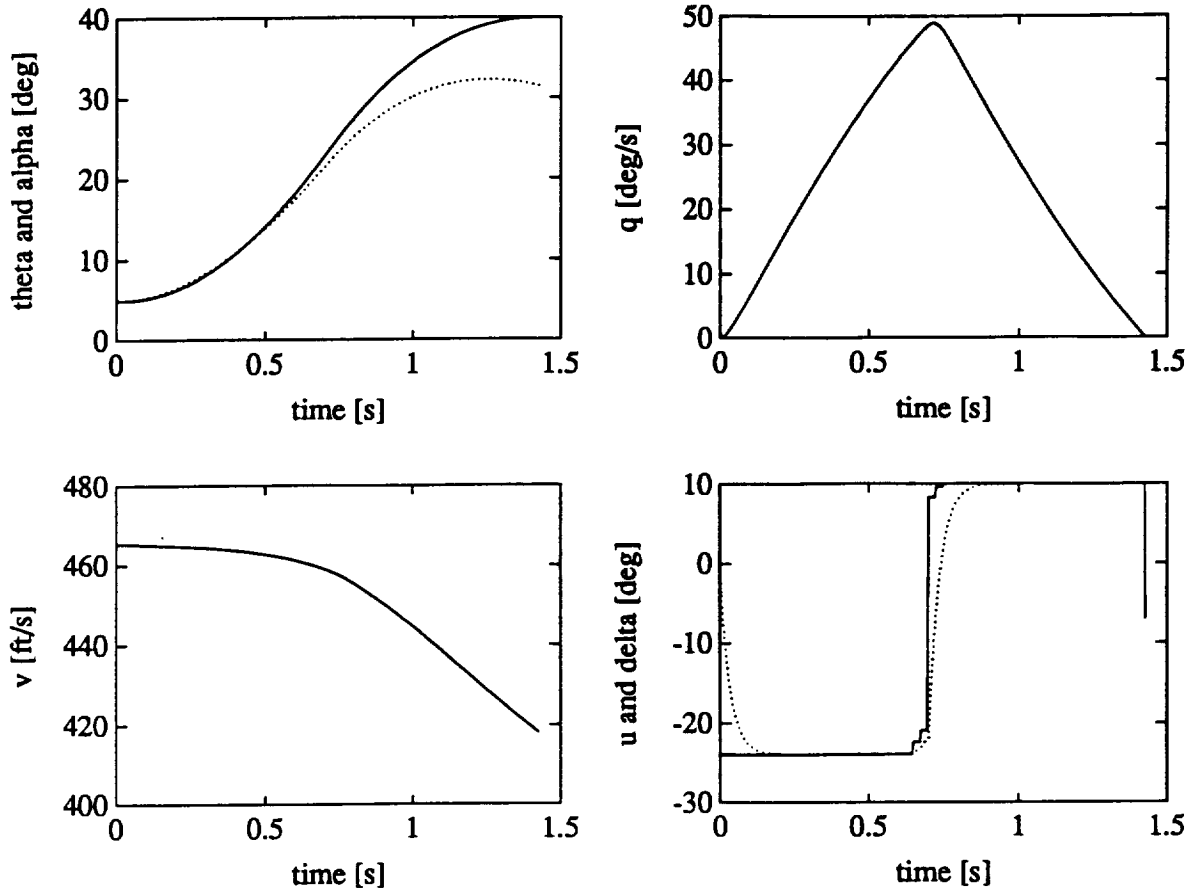


Figure 7. Time-Optimal Maneuver to  $\theta = 40^\circ$ ,  $\alpha \approx 30^\circ$

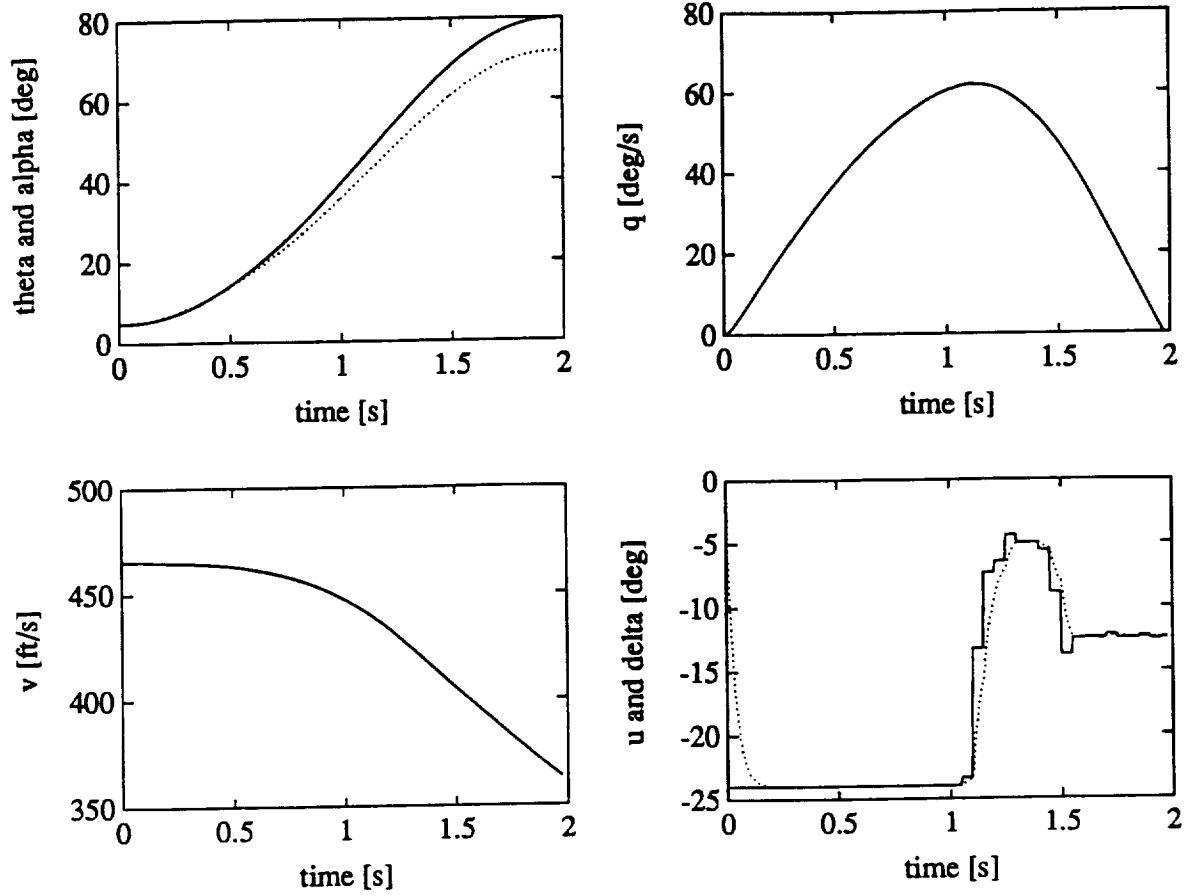


Figure 8. Time-Optimal Manuever to  $\theta = 80^\circ$ ,  $\alpha \approx 72^\circ$

## 4.1 Sliding-Mode Control (SMC)

The sliding-mode control, SMC, is a variable high-speed switching feedback control. The main advantages of SMC are robustness to plant dynamics and disturbances [10-20]. However, SMC may suffer robustness in performance as a result of unknown plant dynamics and control rate or magnitude constraints.

Existence of a sliding mode requires stability of the state trajectory to the sliding surface  $s(\mathbf{x}) = 0$  at least in a neighborhood of  $\{\mathbf{x} | s(\mathbf{x}) = 0\}$ . The largest such neighborhood is called a region of attraction. The existence problem of a sliding mode can be based on the second method of Lyapunov. That is, a general Lyapunov function,  $V(t, \mathbf{x})$ , which is positive definite and has a negative first time derivative in the region of attraction. Consequently, the existence and uniqueness of solutions to SMC results from the method of Filippov, such that [10-13]

$$s(\mathbf{x}) \dot{s}(\mathbf{x}) < 0 . \quad (25)$$

## 4.2 Feedback Linearization

Feedback linearization is an approach to control a nonlinear system by transformation into a fully or partly linear one so that linear control techniques can be applied [13,18]. In this respect, consider the single input, single output nonlinear system

$$\begin{aligned} \dot{\mathbf{x}} &= \mathbf{f}(\mathbf{x}, u) , \\ y &= \mathbf{h}(\mathbf{x}) \end{aligned} \quad (26)$$

where  $\mathbf{x} \in \mathbf{R}^n$ ;  $u, y$  are scalars.

Our objective is to make the output  $y(t)$  follow the desired trajectory  $y_d(t)$  within the bound of the state, where  $y_d(t)$  and its derivatives are assumed to be known and bounded. Here input-output linearization, in which relative degree is less than system dimension  $n$ , is considered. In this case, it is assumed that zero dynamics which is the dynamics of the system subject to the constraint that the output

is zero, must be exponentially minimum phase. The main idea is to repeatedly differentiate the output  $y$  until the output  $y$  is related to the input as follows:

$$\dot{y} = \nabla h(f + gu) = L_f h(x) + L_g h(x) u \quad (27)$$

where  $L_g h(x)$  is a Lie-derivative [13,18].

If  $L_g h(x)$  is not equal to zero for all  $x$  in the neighborhood  $x_0$ , we should differentiate until  $L_g L_f^{r-1} h(x) \neq 0$  for some integer  $r$  which is relative degree of  $r$  of the system. Then the control law

$$u = \frac{1}{L_g L_f^{r-1} h(x)} \left( -L_f^r h(x) + v \right) \quad (28)$$

results in the linear differential relation

$$y^{(r)} = v. \quad (29)$$

When  $r < n$ , there exists a diffeomorphic coordinate transformation  $(\zeta, \eta) = T(x)$  for the normal form

$$\frac{d}{dt} \begin{bmatrix} \zeta_1 \\ \vdots \\ \zeta_{r-1} \\ \zeta_r \end{bmatrix} = \begin{bmatrix} \zeta_2 \\ \vdots \\ \zeta_r \\ a(\zeta, \eta) + b(\zeta, \eta)u \end{bmatrix} \quad (30)$$

$$\dot{\zeta} = w(\zeta, \eta) \quad y = h(x) = \zeta_1 \quad (31)$$

where

$$\zeta = \left[ h \quad L_f h \quad \dots \quad L_f^{r-1} h \right]^T$$

$$\eta = \left[ \eta_1 \quad \dots, \eta_{n-r} \right]^T$$

$$a(\zeta, \eta) = L_f^r h(x) \quad (32)$$

$$b(\zeta, \eta) = L_g L_f^r h(x) \quad (33)$$

Now the control law is

$$u = \frac{1}{b(\zeta, \eta)} [-a(\zeta, \eta) + v] \quad (34)$$

which results in the linear differential relation

$$y^{(r)} = v$$

If

$$v = y_d^{(r)} + \sum_{i=0}^{r-1} -a_i e^{(i)}$$

where  $e = y - y_d$  such that  $p^r + a_{r-1}p^{r-1} + \dots + a_0$  is a Hurwitz polynomial, then the tracking error  $e$  will converge to zero as time  $t$  goes to infinity and the internal state  $\eta$  will be bounded,  $\|\eta\| \leq \delta$ , where  $\delta$  is positive.

For the multi-input, multi-output system

$$\dot{x} = f(x) + g_1(x)u_1 + \dots + g_m(x)u_m$$

or

$$\dot{x} = f(x) + G(x)u \quad (35)$$

$$y = h(x)$$

For some j-th term  $j = 1, \dots, m$

$$\dot{y}_j = L_f h_j + \sum_{i=1}^m (L_{g_i} L_f h_j) u_i \quad (36)$$

If

$$L_{g_i} h_j(x) = 0$$

for all i, we have to differentiate until at least one of the inputs appear in  $y_j^{r_j}$ .

Then

$$y_j^{r_j} = L_f^{r_j} h_j + \sum_{i=1}^m L_{g_i} L_f^{r_j-1} h_j u_i \quad (37)$$

In matrix form

$$y_r = F(x) + B(x) u \quad (38)$$

$$y_r = [y_1^{r_1} \dots y_m^{r_m}]^T \quad (39)$$

where

$$F(x) = [L_f^{r_1} h_1 \dots L_f^{r_m} h_m]^T \quad (40)$$

$$B(x) = \begin{bmatrix} L_{g_1} L_f^{r_1-1} h_1 & \dots & L_{g_m} L_f^{r_1-1} h_1 \\ \vdots & \ddots & \vdots \\ L_{g_1} L_f^{r_m-1} h_m & \dots & L_{g_m} L_f^{r_m-1} h_m \end{bmatrix} \quad (41)$$

If  $E^{-1}(x)$  exists, control law

$$u = -B^{-1}(x) F(x) + B^{-1}(x) v \quad (42)$$

where

$$\mathbf{v} = [v_1 \dots v_m]^T$$

results in

$$\mathbf{y}^r = \mathbf{v} \quad (43)$$

If  $\mathbf{B}^{-1}(\mathbf{x})$  does not exist, we must use another method such as a dynamic-equation algebraic method.

### 4.3 Continuous Sliding-Mode Control with Linearization

In classical SMC, chattering is inevitable due to measurement errors, finite switching time, etc. In this section, the continuous sliding-mode control with I/O linearization is developed, which may have the desirable features of SMC while possibly rejecting the major cause of chatter. For the SISO case the output is obtained after differentiating several times until it is related to the input by  $y^r = L_f^r h(\mathbf{x}) + L_g L_f^{r-1} h(\mathbf{x})u$ . References [21-24] are followed in the approach used here.

Select a sliding surface

$$s = \mathbf{p}^T \mathbf{Y}_{r-1} \quad (44)$$

where

$$\mathbf{p}^T = [p_1 \dots p_r]$$

$$\mathbf{Y}_{r-1} = [e \ \dot{e} \ \dots \ e^{r-1}]^T$$

$$\dot{s} = \mathbf{p}^T \mathbf{Y}_r \quad (45)$$

and

$$\mathbf{Y}_r = [\dot{e} \ \dots \ e^r]^T$$

The sliding conditions evolve from

$$s\dot{s} = \mathbf{sp}^T \mathbf{Y}_r = \mathbf{sp}^T [\dot{e} \dots e^r] \quad (46)$$

$$e^r = y^r - y_d^r = L_f^r h + (L_g L_f^{r-1} h) u - y_d^r \quad (47)$$

Using (47) and (46) results in

$$\begin{aligned} s\dot{s} &= \mathbf{sp}^T \left[ \dot{e} \dots e^{r-1} L_f^r h + (L_g L_f^{r-1} h) u - y_d^r \right]^T \\ &= sp_1 \dot{e} + sp_2 \ddot{e} + \dots + sp_{r-1} e^{r-1} + sp_r \left[ L_f^r h + (L_g L_f^{r-1} h) u - y_d^r \right] \\ &= sp_r L_g L_f^{r-1} h \left\{ u + (sp_r L_g L_f^{r-1} h)^{-1} (sp_1 \dot{e} + sp_2 \ddot{e} + \dots + sp_{r-1} e^{r-1} - sp_r y_d^r) \right\} \end{aligned}$$

If

$$u = - (sp_r L_g L_f^{r-1} h)^{-1} (sp_1 \dot{e} + sp_2 \ddot{e} + \dots + sp_{r-1} e^{r-1} - sp_r y_d^r - sp_r L_g L_f^{r-1} h) \quad (48)$$

$$s\dot{s} = - (sp_r L_g L_f^{r-1} h)^2 < 0 \quad (49)$$

For the multi-input, multi-output case, the attractivity condition for SMC towards  $\mathbf{S} = 0$ ,  $\dot{\mathbf{S}} = 0$  becomes  $\mathbf{S}^T \dot{\mathbf{S}} < 0$ .

Let the sliding surface  $\mathbf{S} = [s_1 \dots s_m]^T$  for some j-th term,  $j = 1, \dots, m$

$$s_j = \sum_{i=0}^{r_j-1} c_{ji} e_j^i \quad (50)$$

$$\begin{aligned}
\dot{s}_j &= e_j^{r_j} + \sum_{i=1}^{r_j-1} c_{j,i-1} e_j^i \\
&= L_f^{r_j} h_j - y_d^{r_j} + \sum_{i=1}^m \left( L_g L_f^{r_j-1} h_j \right) u_i + \sum_{i=1}^{r_j-1} c_{j,i-1} e_j^i
\end{aligned} \tag{51}$$

In the matrix form

$$\mathbf{S} = \begin{bmatrix} \sum_{i=0}^{r_1-1} c_{1,i} e_1^i \\ \vdots \\ \sum_{i=0}^{r_m-1} c_{m,i} e_m^i \end{bmatrix} \triangleq \mathbf{E} = [\mathbf{E}_1 \dots \mathbf{E}_m]^T \tag{52}$$

$$\dot{\mathbf{S}} = \mathbf{e}^r + \mathbf{E}' \tag{53}$$

where

$$\begin{aligned}
\mathbf{e}^r &= [e_1^{r_1} \dots e_m^{r_m}]^T \\
\mathbf{E}' &= \begin{bmatrix} \sum_{i=1}^{r_1-1} c_{1,i-1} e_1^i \\ \vdots \\ \sum_{i=1}^{r_m-1} c_{m,i-1} e_m^i \end{bmatrix}
\end{aligned}$$

Using equation (51), for some  $j$  (53) results in

$$\dot{\mathbf{S}} = L_f^r \mathbf{h} - \mathbf{y}_d^r + \mathbf{E}' + \mathbf{B}u \tag{54}$$

where

$$\mathbf{L}_f^r \mathbf{h} - \mathbf{y}_d^r + \mathbf{E}' = \begin{bmatrix} \mathbf{L}_f^{r_1} \mathbf{h}_1 - \mathbf{y}_{d_1}^{r_1} + \sum_{i=1}^{r_1-1} c_{1,i-1} \mathbf{e}_1^i \\ \vdots \\ \mathbf{L}_f^{r_m} \mathbf{h}_m - \mathbf{y}_{d_m}^{r_m} + \sum_{i=1}^{r_m-1} c_{m,i-1} \mathbf{e}_m^i \end{bmatrix} \quad (55)$$

$$\mathbf{y}^r = \begin{bmatrix} \mathbf{y}_{d_1}^{r_1} & \dots & \mathbf{y}_{d_m}^{r_m} \end{bmatrix}^T \quad (56)$$

$$\mathbf{E}' = \begin{bmatrix} \mathbf{E}'_1 & \mathbf{E}'_2 & \dots & \mathbf{E}'_m \end{bmatrix}^T \quad (57)$$

$$\mathbf{E}'_j = \sum_{i=1}^{r_j-1} c_{j,i-1} \mathbf{e}_j^i \quad j = 1, \dots, m \quad (58)$$

$$\mathbf{u} = [u_1 \dots u_m]^T.$$

$\mathbf{B}$  is the same as equation (41). Therefore, sliding condition

$$\begin{aligned} \mathbf{S}^T \dot{\mathbf{S}} &= \mathbf{E}^T (\mathbf{L}_f^r \mathbf{h} - \mathbf{y}_d^r + \mathbf{E}') + \mathbf{E}^T \mathbf{B} \mathbf{u} \\ &= \mathbf{E}^T \mathbf{B} \left\{ \mathbf{u} + \frac{(\mathbf{E}^T \mathbf{B})^{-T}}{|\mathbf{E}^T \mathbf{B}|^2} \mathbf{E}^T (\mathbf{L}_f^r \mathbf{h} - \mathbf{y}_d^r + \mathbf{E}') \right\} \end{aligned} \quad (59)$$

$$\mathbf{u} = \frac{(\mathbf{E}^T \mathbf{B})^{-T}}{|\mathbf{E}^T \mathbf{B}|^2} \mathbf{E}^T (\mathbf{L}_f^r \mathbf{h} - \mathbf{y}_d^r + \mathbf{E}') - \mathbf{K} (\mathbf{E}^T \mathbf{B})^T$$

where

$\mathbf{K}$  is positive definite matrix, then

$$\mathbf{S}^T \dot{\mathbf{S}} = -\mathbf{E}^T \mathbf{B} \mathbf{K} (\mathbf{E}^T \mathbf{B})^T < 0 \quad (60)$$

## 4.4 Simulation

The plant is the simplified second-order longitudinal motion of a high-alpha airplane [1] with

$$\begin{aligned}\dot{\alpha} &= 9.168 c_z(\alpha) + q - 1.8366(\delta_e + 7) + 7.361904 \\ \dot{q} &= 5.73(C_{m_{\dot{\alpha}}}\alpha + C_{m_{\delta_e}}\delta_e) + 2.865\end{aligned}\tag{61}$$

where  $\alpha$  is the angle of attack in degrees,  $q$  is the pitch rate in degrees per second, and  $\delta_e$  is the elevator control in degrees.

$$C_{M_{\dot{\alpha}}} = -1, \quad C_{m_{\delta_e}} = -1.5$$

and

$$c_z(\alpha) = \begin{cases} -0.07378494 \alpha, & \alpha \leq 14.36 \\ 0.09722 \alpha^2 - 2.8653 \alpha + 20.03846, & 14.36 \leq \alpha \leq 15.6 \\ -0.01971 \alpha^2 + 0.74391 \alpha - 7.80753, & 15.6 \leq \alpha \leq 19.6 \\ -0.47333 - 0.01667 \alpha, & 19.6 \leq \alpha \leq 28 \end{cases}$$

Let  $x_1 = \alpha$ ,  $x_2 = q$ , and the output  $y = \alpha$ , then

$$\dot{\mathbf{x}} = \begin{bmatrix} \dot{x}_1 \\ \dot{x}_2 \end{bmatrix} = \mathbf{f}(\mathbf{x}) + \mathbf{g} \delta_e\tag{62}$$

where

$$\mathbf{g}^T = [-1.8366 \quad -8.595].$$

Uncertainty in  $\mathbf{f}$  and  $\mathbf{g}$  were considered as Gaussian noises with variance of unity.

Here, for convenience and smoothness, we let the desired trajectory

$$y_d = \alpha_{\text{desired}} = (A - \alpha_o) e^{-\lambda t} - (A - 2\alpha_o) e^{-\lambda t}\tag{63}$$

where

$$A = 18^\circ$$

$$\alpha_o = \text{the equilibrium value with } [\alpha_o \ q_o] = [3.20444632 \ 0]$$

$$\delta_e = -1.8029642$$

$$\lambda_1 = 5, \quad \lambda_2 = -1$$

Here, it was assumed that

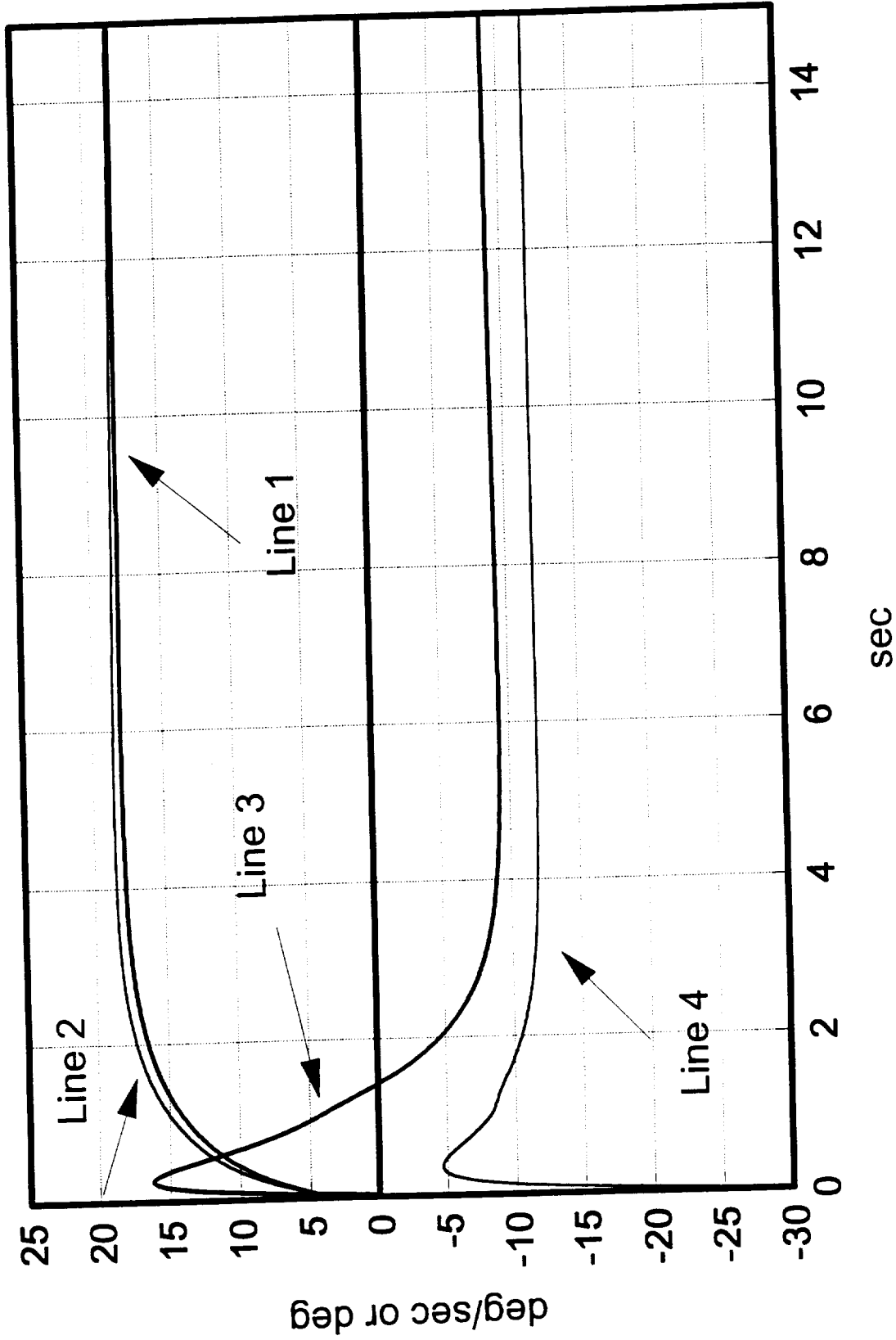
$$\begin{aligned} \dot{e} &= \dot{y} - \dot{y}_d \\ v &= \dot{y}_d + k + I \int_0^t e dt + k_1 e \end{aligned} \tag{64}$$

where  $k_1 = -16$ ,  $k = 10$ , and  $I = -164$  so that the tracking error will be reduced with a damping ratio 0.617 and natural frequency 12.96 rad/sec.

Figures 9 to 14 show the simulated feedback-linearized controlled responses for a change in angle of attack  $\alpha$  from  $0^\circ$  to  $18^\circ$  in a few seconds according to command (63). These use the control of (64) with  $k = I = 0$  for Figs. 9 and 10 and without uncertainty and disturbance for Figs. 9 and 11. Figures 13 and 14 use SMC with linearization. For SMC with linearization, the sliding surface is given by  $s = p_1 e = p_1 (y - y_d)$  where  $p_1 = 1$ . Using equation (48) and (62), the control input is  $u = -g_1^{-1} (f_1 - \dot{y}_d) - s p_1 g_1$ . The last two figures demonstrate the success of SMC with feedback linearization (nonlinear control) relative to the other runs. The constant affine term, derivative, and integral terms are all found to be beneficial for both cases. The nonlinear control (NLC) magnitude, however, is the only one within the physical constraints when uncertainty and disturbance is considered.

It must be realized that this is only a first study of a single sliding-mode control used in conjunction with feedback linearization. It must be studied with the more complex model for larger variations in angle of attack where further dynamic uncertainty is considered along with control rate and acceleration constraints. In any event, such controllers can be used for comparison with more robust nonlinear controllers and linear controllers.

# Without I

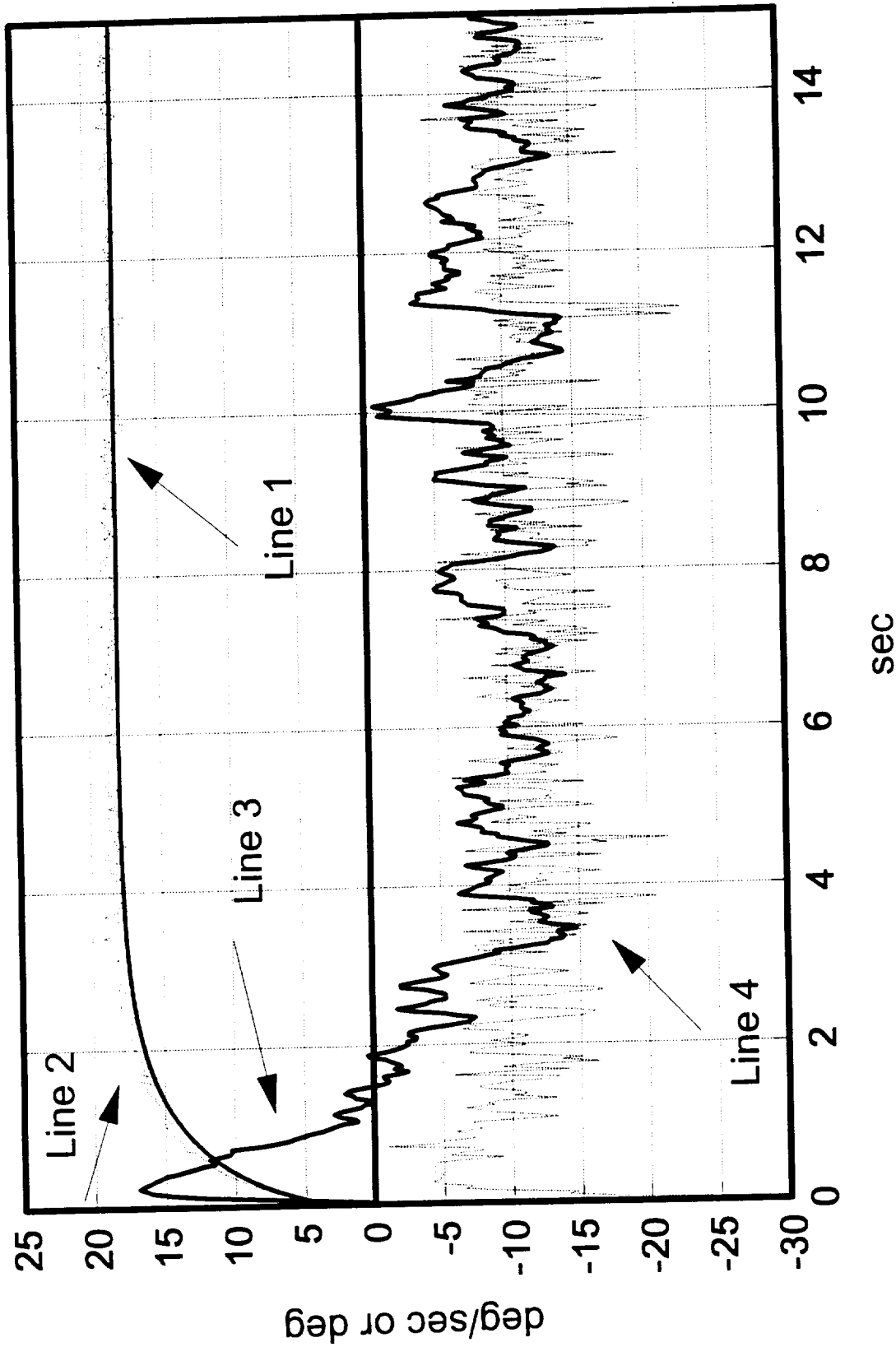


Line 1: Desired angle of attack      Line 2: Angle of attack (deg)

Line 3: pitch rate (deg/sec)      Line 4: Elevator angle (deg)

Figure 9. Feedback-Linearized Control Without Integral Term

# Without I, With disturbance

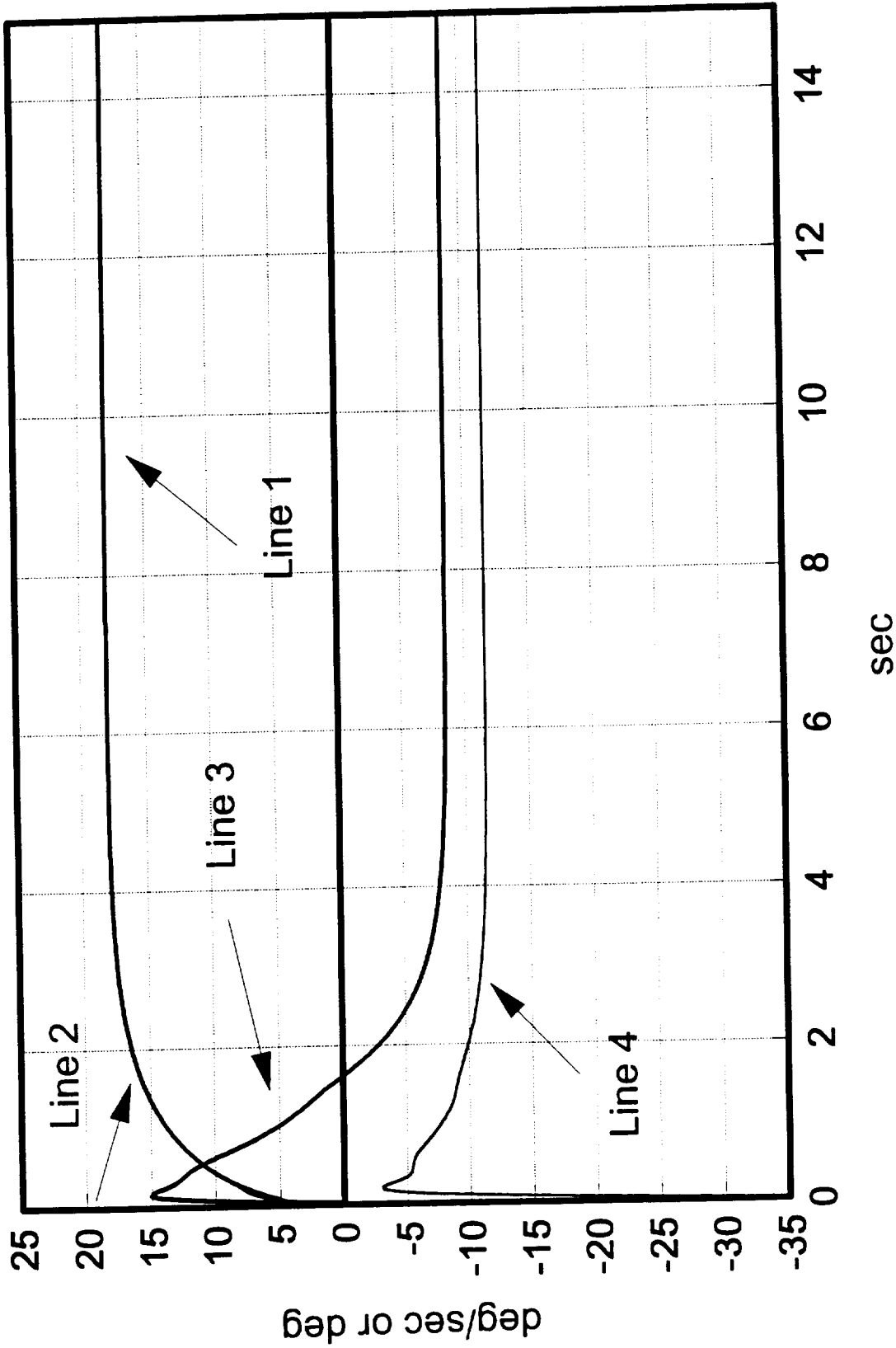


Line 1: Desired angle of attack      Line 2: Angle of attack (deg)

Line 3: pitch rate (deg/sec)      Line 4: Elevator angle (deg)

Figure 10. Feedback-Linearized Control Without Integral Term With Disturbance

With I

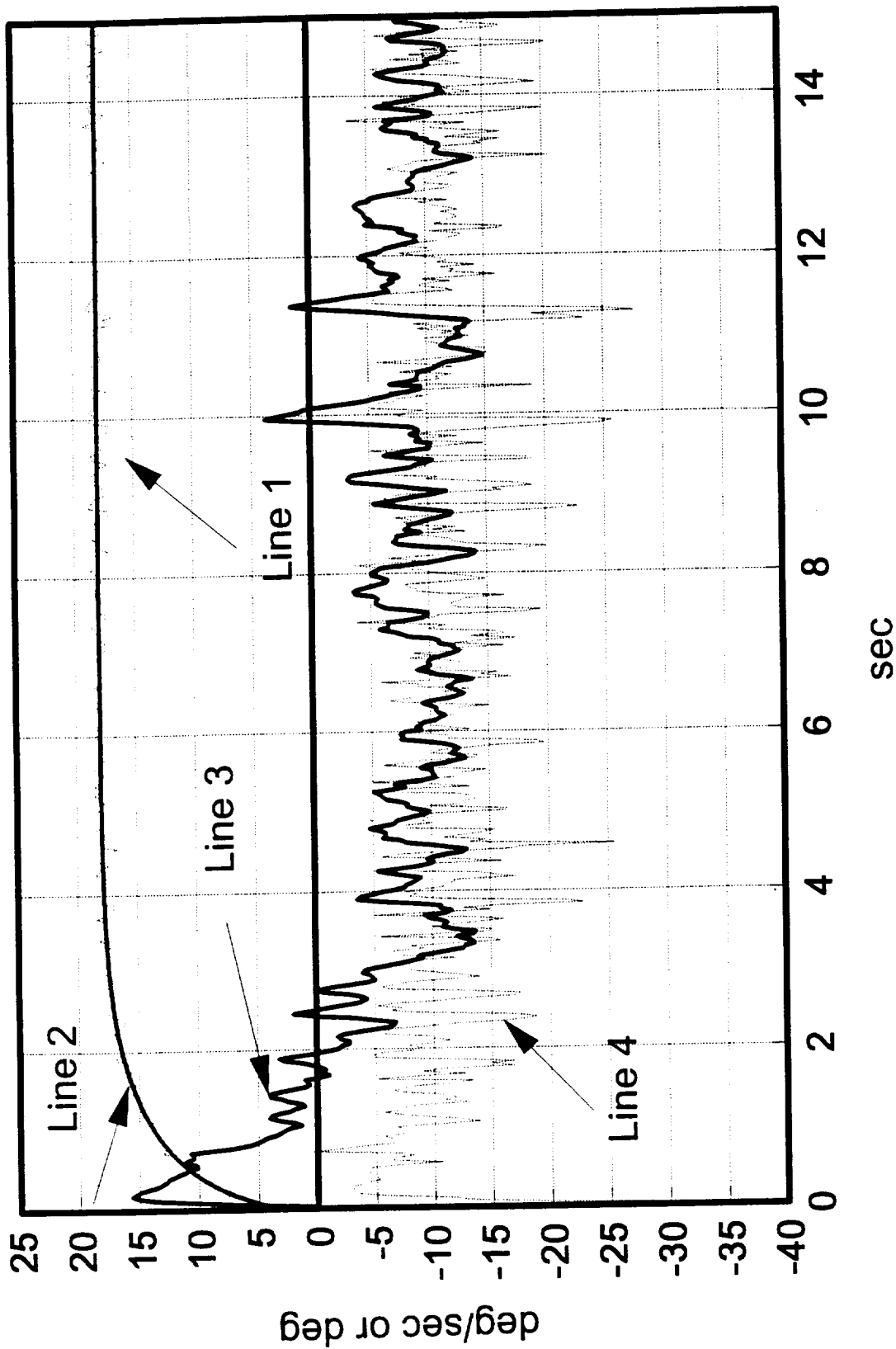


Line 1:Desired angle of attack      Line 2:Angle of attack (deg)

Line 3:pitch rate (deg/sec)      Line 4:Elevator angle (deg)

Figure 11. Feedback-Linearized Control With Integral Term

# With I, With disturbance

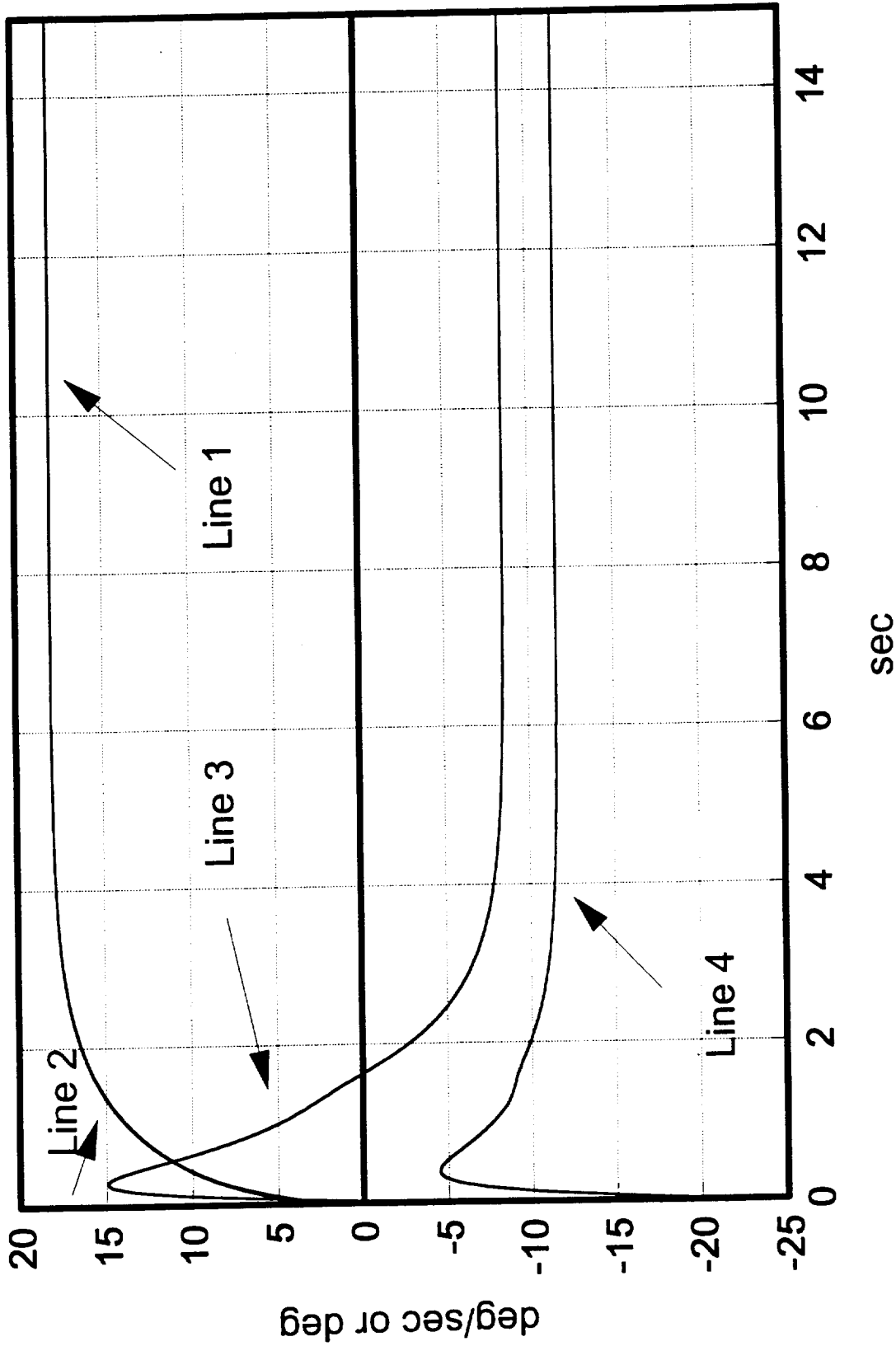


Line 1: Desired angle of attack      Line 2: Angle of attack (deg)

Line 3: pitch rate (deg/sec)      Line 4: Elevator angle (deg)

Figure 12. Feedback-Linearized Control With Integral Term and Disturbance

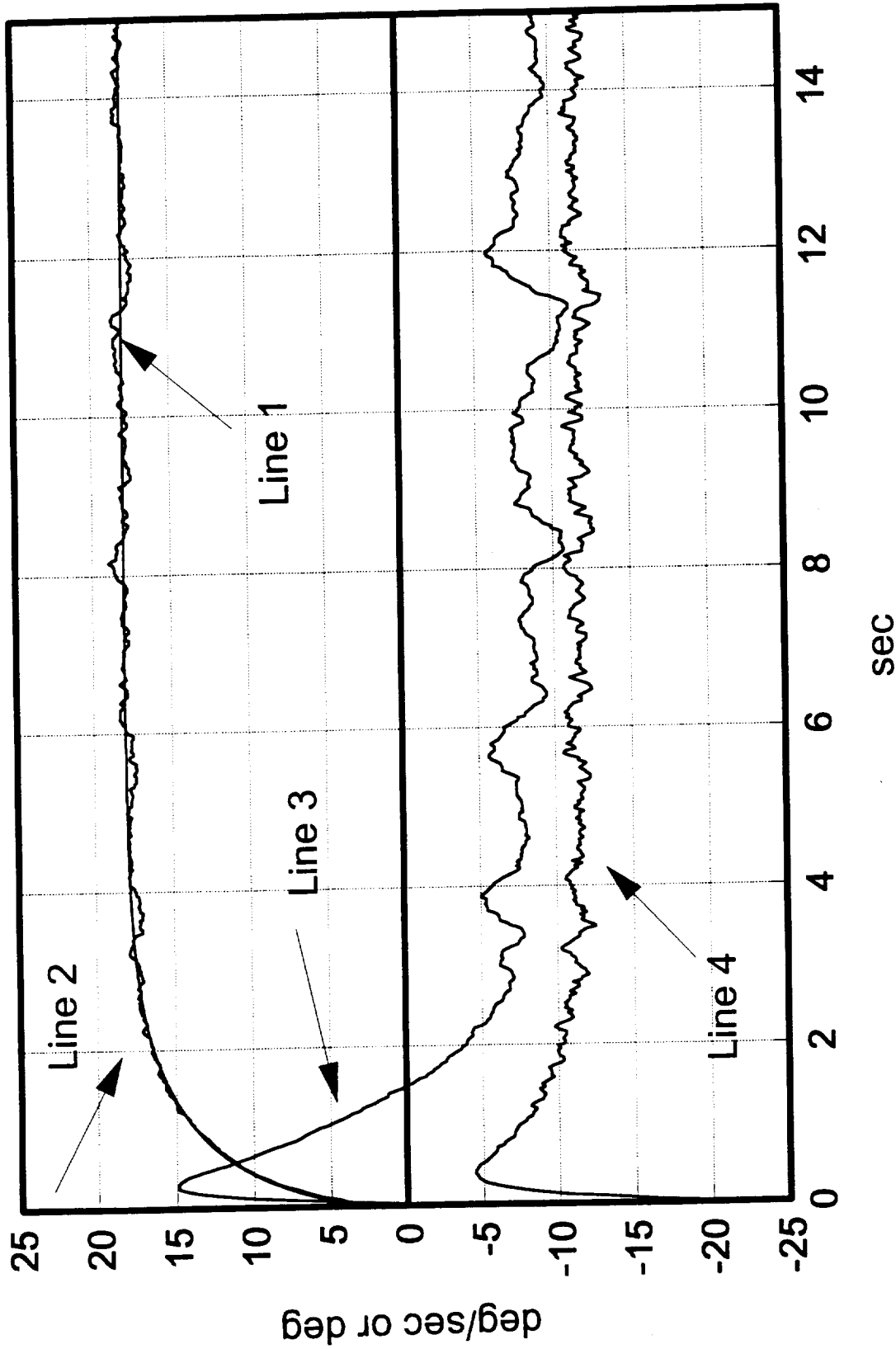
# using SMC



Line 1: Desired angle of attack      Line 2: Angle of attack (deg)  
Line 3: pitch rate (deg/sec)      Line 4: Elevator angle (deg)

Figure 13. Sliding-Mode Control (SMC) With Feedback-Linearization (FL)

# using SMC with disturbance



Line 1: Desired angle of attack      Line 2: Angle of attack (deg)

Line 3: pitch rate (deg/sec)      Line 4: Elevator angle (deg)

Figure 14. SMC-FL Control With Disturbance

## 5. OTHER PRELIMINARY STUDIES

### 5.1 Bilinear-Based Adaptive Control

Bilinear systems (i.e., systems linear in state, linear in control but not jointly linear) represent perhaps the simplest class of nonlinear systems and, indeed, considers the first nonlinear terms in the Taylor series approximation beyond linearization [4]. Bilinear systems (BLS) may be further justified for aircraft dynamic approximation beyond conventional linearized models since lift and drag aerodynamic stability derivatives do depend on control surface variation. For high-performance aircraft using more control, such parametric control terms become more dominant, lead to improved controllability and performance, and here the BLS becomes a first natural approximation beyond linear systems. Indeed, linear analysis fails to predict the desired performance gains and may fail to lead to a stabilizing design for sufficiently large rapid maneuvers. While analytical results for nonlinear systems are somewhat rare, a considerable base for analysis and design has been developed for BLS [4].

The MAC design studied in Section 2 uses a generalization of bilinear terms to compute a nonlinear model-based adaptive controller. Further analysis will consider the effectiveness of such bilinear-based control. But here we consider another approach which could lead to a simple nonlinear feedback configuration or could be used as a basis for nonlinear PIF control.

As a BLS model reference consider the discrete equation

$$\mathbf{x}_{k+1} = \mathbf{A}_k \mathbf{x}_k + \mathbf{B}_k \mathbf{u}_k + \sum_{i=1}^m \mathbf{N}_{ki} \mathbf{u}_{ki} \mathbf{x}_k$$

where, for example,  $\mathbf{x}^T = [\alpha \ q \ \theta \ v]$  is comprised of angle of attack, pitch rate, pitch, and air speed. The control  $\mathbf{u}$  may include, for example, stabilator and thrust vector mechanisms with an error vector  $\mathbf{e}_k$  taken about some desired trim state or trajectory.

For a first design approach select a quadratic Lyapunov function in  $\mathbf{e}_k$  (and possibly control rate of change). An effective stabilizing controller can then be generated in terms of quadratic and linear

feedback terms — the quadratic term being most effective for large errors and the traditional linear feedback most effective for small errors [4]. Detailed design and simulation are in progress.

## 5.2 Neural-Net-Based Control

A preliminary study has been started on dynamic aircraft modeling and control by means of artificial neural networks. One approach utilizes the time-optimal control study summarized in Section 3.

The main idea of the approach is to utilize the approximating capabilities of neural networks to extract the closed-loop information from open-loop optimal trajectories. The synthesis of the feedback time-optimal controller for a general nonlinear plant is very often untractable from the analytical point of view. On the other hand, powerful theory and many efficient numerical algorithms exist for the open-loop problem that allow us to calculate optimal trajectories for given initial and final constraints. Those trajectories, however, contain information about optimal feedback. For a sufficiently regular optimal control problem with integral quality index the principle of optimality assures that an instantaneous value of control is a function of the current state, unique up to a set of measure zero. Hence, it may be written that

$$u^{opt}(t) = g(x(t))$$

Each point of an optimal trajectory may be viewed as a point on a hypersurface representing a mapping  $g$ . If sufficiently many time-optimal trajectories are collected and sampled the mapping  $g$  may be reconstructed. We propose to use multilayered neural networks to do so. Their capabilities as function approximators are widely used in the system and control area to extract complex nonlinear functions from discrete measurement data. The theoretical basis for those applications is a result stating that given any continuous finite-dimensional function defined over a compact set there exists a feed-forward neural network with one hidden layer which approximates the function arbitrarily closely in a uniform sense. Since continuous-function compact sets are dense in  $L^2$ , a network approximating optimal

control mapping  $g$  in a mean-square sense is guaranteed to exist, and one of the training algorithms minimizing the mean-square error may be used. The advantage of this approach is that instead of solving the nonlinear optimal feedback synthesis problem we deal with an easier problem of calculating open-loop trajectories for different initial conditions.

For the second-order model described above time-optimal control strategies were approximated using a simple single-layer neural net. Time-optimal transition was considered to the equilibrium points corresponding to angle attack equal 0, 5, 10, 15, and 20. First five separate neural networks were trained to approximate the time-optimal strategies for these five target points. To train a network to approximate the mapping

$$\delta^{\text{opt}} = g^{\text{opt}}(\alpha, q)$$

a set of open-loop optimizations was performed for different starting points. Then resulting time-optimal trajectories were sampled every 0.05 s. For the model in question the time-optimal control is of a bang-bang type. Training data for the three typical cases is shown for the second-order nonlinear model in Fig. 15 with "\*" signs corresponding to the control value 0 and "+" signs corresponding to value of -20. Figure 15 requires some comment.

The data was used to train five neural networks with two inputs ( $\alpha$  and  $q$ ), one output ( $\delta$ ), and one hidden layer of 20 neurons. Sigmoid neurons were used in both hidden and output layer. Each network was trained off-line and training lasted 2000 iterations (epochs). In each case, very good approximation of function was obtained.

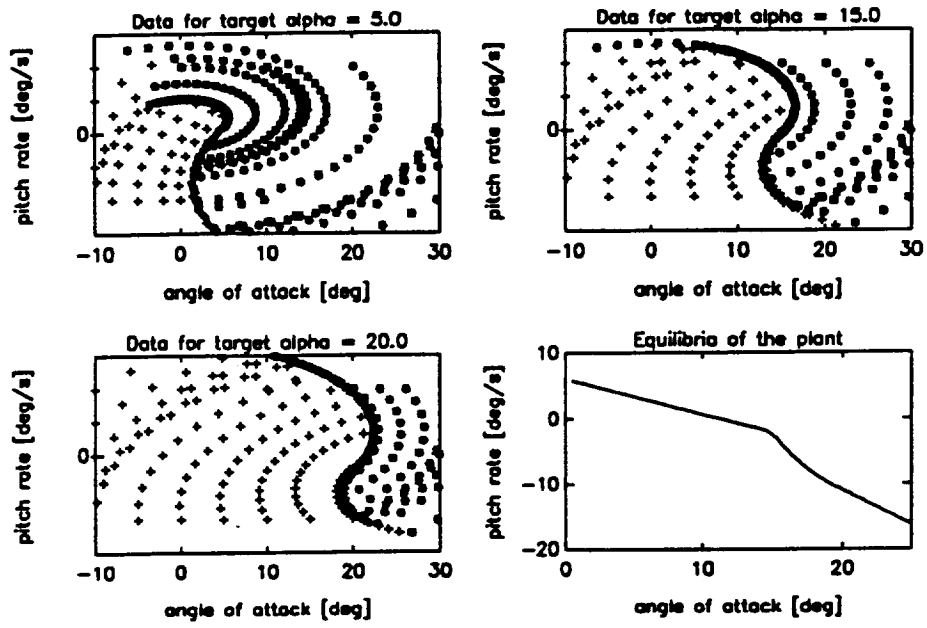


Figure 15. Training Data for Three Different Values of Target  $\alpha$  with the Set of Equilibria of the System

## 6. REFERENCES

- [1] H. Stalford, W.T. Bauman, F.E. Garret, and T.L. Herdman, "Accurate Modeling of Nonlinear Systems using Volterra Series Submodels," *Proc. American Control Conf.*, Minneapolis, 886-891, 1987.
- [2] A.J. Ostroff, "Application of Variable-gain Output Feedback for High-alpha Control," *AIAA Guidance, Nav. & Control Conf.* (Paper No. 89-3576), Boston, 1989.
- [3] R.R. Mohler, ed., Annual Report on "Nonlinear Stability and Control Study of Highly Maneuverable High Performance Aircraft," OSU ECE Report NASA 9101, August 1991.
- [4] R.R. Mohler, *Nonlinear Systems: V. 2 Applications to Bilinear Control*, Prentice Hall, 1991.
- [5] S.F. Moon, "Optimal Control of Bilinear Systems and Systems Linear in Control," Ph.D. dissertation, The University of New Mexico, 1969.
- [6] H. Hermes and J.P. Lasalle, *Functional Analysis and Time Optimal Control*, Academic Press, 1969.
- [7] W. Hejzo, *Theory of Time Optimal Control and Its Applications*, PWN, Warsaw, 1990 (in Polish).
- [8] R.R. Mohler, ed., Semi-Annual Report on "Nonlinear Stability and Control Study of Highly Maneuverable High Performance Aircraft," OSU-ECE Report NASA 9201, Corvallis, OR, February 1992.
- [9] R.R. Mohler, *Nonlinear Systems: Vol. 1 Dynamics and Control*, Englewood Cliffs, NJ, 1991.
- [10] R.A. DeCarlo, S.H. Zak, and G.P. Matthews, "Variable-Structure Control of Nonlinear Multivariable Systems: A Tutorial," *Proc. IEEE* 76, 212-232, 1988.
- [11] A.F. Filippov, "Differential Equations with Discontinuous Right-Hand Sides," *Am. Math. Soc. Trans.* 62, 199, 1964.
- [12] L.W. Chang, "A MIMO Sliding Control with a Second-Order Sliding Condition," *ASME WAM* (Paper No. 90-WA/DSC-5) Dallas, TX, 1990.
- [13] A. Isidori, *Nonlinear Control Systems: An Introduction*, Springer, New York, 1985.

- [14] J.J. Slotine, "Sliding Controller Design for Nonlinear Systems," *Int. J. Control* 40, 421-434, 1984.
- [15] H. Elmali and N. Olgac, "Theory and Implementation of Sliding Mode Control with Perturbation Estimation," *Proc. IEEE Int'l Conf. Robotics & Automation*, Nice, France, May 1992.
- [16] J.J. Slotine and S.S. Sastry, "Tracking Control of Non-Linear Systems Using Sliding Surfaces, with Application to Robot Manipulators," *Int. J. Control* 38, 465-492, 1983.
- [17] V.I. Utkin, *Sliding Modes and Their Application in Variable Structure Systems*, MIT Press, Moscow, 1978.
- [18] J.J. Slotine and Weiping Li, *Applied Nonlinear Control*, Prentice-Hall, Englewood Cliffs, NJ, 1991.
- [19] F. Zhou, and D. Fisher, "Continuous Sliding Mode Control," *Int. J. Control* 55, 313-327, 1992.
- [20] H. Elmali and N. Olgac, "Robust Output Tracking Control of Nonlinear MIMO Systems via Sliding Mode Technique," *Automatica* 28, 145-151, 1992.
- [21] S. Behtash, "Robust Output Tracking for Nonlinear System," *Int. J. Control* 51, 1381-1407, 1990.
- [22] M.J. Corless and G. Leitmann, "Continuous State Feedback Guaranteeing Uniform Ultimate Boundness for Uncertain Dynamic System," *IEEE Trans. Automatic Control* AC-26, 1139-1144, 1981.
- [23] B.R. Barmish, M. Corless, and G. Leitmann, "A New Class of Stabilizing Controllers for Uncertain Dynamical System," *SIAM J. Control and Optimization* 21, 246-255, 1983.
- [24] S. Gutman, "Uncertain Dynamic System-Lyapunov min-max Approach," *IEEE Trans. Automatic Control* AC-24, 437-443, 1979.

---

**APPENDIX A**

**Project Publications**

## PROJECT PUBLICATIONS

(Supported Wholly or in Part by NASA Grant)

1. R.R. Zakrzewski and R.R. Mohler, "On Nonlinear Model Algorithm Controller Design," *Proceedings*, IFIP Conf. Sys. Modeling and Optimiz., Zurich, 1991. (See Appendix B)
2. R.R. Mohler, V. Rajkumar, and R.R. Zakrzewski, "Nonlinear Time-Series Based Adaptive Control Applications," *Proceedings*, IEEE Conf. Decision & Control, Brighton, 1991.
3. R.R. Mohler, *Nonlinear Systems: Vol. 2 Applications to Bilinear Control*, Prentice Hall, Englewood Cliffs, NJ, 1991.
4. R.R. Mohler, V. Rajkumar, and R.R. Zakrzewski, "On Discrete Nonlinear Self-Tuning Control," *Proceedings*, Korean Control Conf., Seoul, 1991.
5. R.R. Mohler, R. Zakrzewski, S. Cho, and C. Koo, "New Results on Nonlinear Adaptive High Alpha Control," Comcon 3, Victoria, 1991.
6. J.E. Kurek, "Analysis of Nonlinear Stability Using Robust Stability Analysis for Linear Systems," submitted, 1992.
7. R.R. Mohler and R.R. Zakrzewski, "Suboptimal Intelligent Control with High Alpha Aircraft Application," to appear.

## **APPENDIX B**

### **On Nonlinear Model Algorithmic Controller Design**

## ON NONLINEAR MODEL ALGORITHMIC CONTROLLER DESIGN

R.R. Zakrzewski and R.R. Mohler  
Oregon State University  
Department of Electrical and Computer Engineering  
Corvallis, OR 97331  
USA

### 1. INTRODUCTION

Two nonlinear algorithmic controllers, MAC, are studied here. One uses a block-canceling Volterra approximation, and the other MAC consists of solving an approximating polynomial time series in state and control. Both methods synthesize discrete control sequences and are applied successfully to the control of a simple nonlinear longitudinal aircraft model for large variations in angle of attack.

The Volterra-series approach used here was introduced by Modyaev and Averina [1], and a form of inverse generating control according to an assumed structure is presented by Harris [2]. This work formed the basis for the methods used here. The high angle-of-attack aircraft model derived by Stalford, et al. [3] was the plant simulated for the MAC application. In many traditional design studies, a sequence of linearized perturbation models are derived for different equilibrium flight conditions with linear controllers appropriately derived. Linear adaptive control can be derived according to nonlinear gain scheduling of the control law. A highly successful version of such control, which includes proportional plus integral plus filter (PIF) terms, is presented by Ostroff [4,5]. However, such designs usually require a large number of set-point design computations, and may have stability problems for large fast changes in angle of attack and/or mach number.

For generation of the nonlinear control, a nonlinear time-series based model reference is used. In order to identify such model, experimental data was collected for angle of attack ( $\alpha$ ) and pitch rate ( $q$ ) subject to random steps of control

(stabilator,  $\delta$ ). To capture such phenomena as limit cycles in the data the steps were rather long (40 s). There were 64 such steps with time discretization of 0.1 s resulting in 25,600 points in a state plane for 64 values of control.

For a least-squares simulated data fit, the following approximation was surprisingly accurate:

$$\begin{aligned}
 \alpha(k+1) &= p_{1\alpha}\alpha(k) + p_{2\alpha}\alpha^2(k) + p_{3\alpha}\alpha^3(k) + \\
 & p_{4\alpha}q(k) + p_{5\alpha}q(k)\alpha(k) + p_{6\alpha}q(k)\alpha^2(k) + p_{7\alpha}q(k)\alpha^3(k) + \\
 & p_{8\alpha}u(k) + p_{9\alpha}u(k)\alpha(k) + p_{10\alpha}u(k)\alpha^2(k) + p_{11\alpha}u(k)\alpha^3(k) + p_{12\alpha} \quad (1) \\
 q(k+1) &= p_{1q}\alpha(k) + p_{2q}\alpha^2(k) + p_{3q}\alpha^3(k) + \\
 & p_{4q}q(k) + p_{5q}q(k)\alpha(k) + p_{6q}q(k)\alpha^2(k) + p_{7q}q(k)\alpha^3(k) + \\
 & p_{8q}qu(k) + p_{9q}u(k)\alpha(k) + p_{10q}u(k)\alpha^2(k) + p_{11q}u(k)\alpha^3(k) + p_{12q}
 \end{aligned}$$

Even limit cycles are accurately rendered by this model, as well as the stable zone behavior, although large discrepancies occur when the control values are close to the stable/unstable zones border.

## 2. ADAPTIVE CONTROL APPROACHES

### 2.1 Nonlinear Volterra-Based Control

Here, as in [6], the Volterra series serves as a conceptual starting point for a nonlinear time series base control. Continuous time controllers based on Volterra series were systematically developed in [7] with formulae for the controller's kernels given those of the plant and of the desired feedback system. In particular, the problem of so-called exact feedback linearization was solved here. However, those formulae may be of limited practical value because of the properties of Volterra series under feedback. The problem is that even finite (e.g., second order) Volterra series of the open loop results in infinite Volterra series of the closed loop. This makes it necessary for the controller to include theoretically an infinite number of

compensating terms even for a quadratic system. The same problem for the discrete time systems was treated in [1] with multidimensional Z transforms to derive the set of formulae equivalent to those for so-called exact feedback linearization [8]. However, they also provided a very elegant transformation of which results in a controller requiring only as many Volterra terms as there are in the assumed plant.

One attractive feature of this controller is that its structure makes it possible to utilize it not only with models represented in the form of Volterra series, but in fact with any model with easily divided linear and nonlinear parts of the dynamic equations such as (2) above.

The following algorithm results:

- a) according to the linear part of the plant, calculate the linear control  $u_L(k)$
- b) calculate the predicted value of the output at the moment  $k$

$$\hat{y}(k) = L(y(k-1), \dots, y(k-M), u(k-1), \dots, u(k-M)) \\ N(y(k-1), \dots, y(k-M), u(k-1), \dots, u(k-M))$$

- c) solve the "linearizing" control equation for  $x(k)$  such that

$$N(\hat{y}(k), y(k-1), \dots, y(k-M+1), u_L(k) - x(k), u(k-1), \dots, u(k-M+1)) = \\ = L(x(k), x(k-1), \dots, x(k-M+1), \hat{y}(k), y(k-1), \dots, y(k-M+1))$$

- 3) calculate the control by

$$u(k) = U_L(k) - x(k)$$

This algorithm becomes a sort of prediction controller which tries to estimate the effects of the previous controls knowing the previous values of outputs and then to adjust the current value of control so that the nonlinear part of predicted output is canceled.

This discrete time nonlinear  $\alpha$  control algorithm is generated according to an off-line identification of model (1) with a nonlinear aircraft simulation based on [3]. Also, a linear controller was designed according to the linear parts of (1)-(3).

The design was performed to obtain the closed loop model reference behavior of the form

$$G(z) = 0.05/(z^2 - 1.6z + 0.65)$$

In order not to cancel the zero of the plant, the observer polynomial  $(z-0.7)$  was introduced. The algorithm for the control value  $u(k)$  is as follows. First the estimate of the output at moment  $k$  is calculated from (1) with  $k$  replaced by  $k-1$ .

Then it can be shown that the control becomes

$$u(k) + \frac{p_{8\alpha} u_L(k) - (p_{2\alpha} \hat{\alpha}^2 + p_{3\alpha} \hat{\alpha}^3 + p_{5\alpha} \hat{\alpha} \hat{q} + p_{6\alpha} \hat{q} \hat{\alpha}^2 + p_{7\alpha} \hat{q} \hat{\alpha}^3 + p_{12\alpha})}{(p_{8\alpha} + p_{9\alpha} \hat{\alpha} + p_{10\alpha} \hat{\alpha}^2 + p_{11\alpha} \hat{\alpha}^3)} \quad (4)$$

with  $\hat{\alpha}(k)$  and  $\hat{q}(k)$  designating estimates taken from (1). It is seen that if there are no nonlinearities in the model the control reduces to a regular linear controller  $u = u_L$ .

Simulations were run to test the controller performance especially in the unstable range of angle of attack. The system is successfully stabilized and the transients are very smooth and without significant overshoots for the nonlinear control as demonstrated by Figure 1a. By different choice of the reference model it is possible to obtain much faster, but at the same time much more "nervous" transients. The elevator control is also relatively smooth and within the range corresponding to the terminal equilibria. As can be seen from Figure 1b, the similar linear control is unstable.

## 2.2 On-Line Adaptive MAC Algorithm

Model algorithmic control (MAC), described for example in [2], consists of solving the model equation for the value of control necessary to obtain required value of output. Usually this desired output trajectory is generated from the setpoint by means of a reference model. In case this model is linear, the algorithm in essence becomes a linearizing one.

Here, the controlled output is assumed to be the angle of attack such that the reference equation becomes:

$$\alpha_{ref}(k+1) = \hat{\alpha}_{mod}(k+1) + (\alpha(k-1) - \alpha_{mod}(k-1)) \quad (5)$$

with

$$\begin{aligned} \hat{\alpha}_{mod}(k+1) &= p_a^T \hat{\phi}(k) \\ \hat{\phi}(k) &= [\hat{\alpha}, \hat{\alpha}^2, \hat{\alpha}^3, q, q\hat{\alpha}, q\hat{\alpha}^2, q\hat{\alpha}^3, u, u\hat{\alpha}, u\hat{\alpha}^2, u\hat{\alpha}^3, 1]^T(k) \\ \hat{\alpha}(k) &= p_a^T \phi(k-1) + (\alpha(k-1) - \alpha_{mod}(k-1)) \\ \hat{q}(k) &= p_q^T \phi(k-1) + (q(k-1) - q_{mod}(k-1)) \end{aligned}$$

The controller is assumed to know the values of angle of attack and of pitch rate at the moment  $k-1$ . Then it estimates their current values  $\alpha(k)$  and  $q(k)$  taking into consideration previous prediction errors and based on them it calculates the control required to achieve  $\alpha_{ref}$  at the moment  $k+1$ . The value of control is found as:

$$u(k) = \frac{\bar{\alpha}_r - p_{1\alpha}\hat{\alpha} - p_{2\alpha}\hat{\alpha}^2 - p_{3\alpha}\hat{\alpha}^3 - p_{4\alpha}\hat{q} - p_{5\alpha}\hat{q}\hat{\alpha} - p_{6\alpha}\hat{q}\hat{\alpha}^2 - p_{7\alpha}\hat{q}\hat{\alpha}^3 - p_{12\alpha}}{p_{8\alpha} + p_{9\alpha}\hat{\alpha} + p_{10\alpha}\hat{\alpha}^2 + p_{11\alpha}\hat{\alpha}^3} \quad (6)$$

where

$$\bar{\alpha}_r = \alpha_{ref}(k+1) - (\alpha(k-1) - \alpha_{mod}(k-1))$$

and  $\hat{\alpha} = \hat{\alpha}(k)$ ,  $\hat{q} = \hat{q}(k)$  as described above.

The results of the simulations are seen in Figures 2a,b. The reference trajectory was chosen to be  $1/z^2 - 1.6z + 0.65$ . The actual output of the plant is seen to follow the reference very closely, even though the region of operation was that of the most severe nonlinearities. The control action is also remarkably smooth.

The discrete time nonlinear state space model (1) describes the behavior of the complex nonlinear plant quite accurately in the entire region of operation. In practice, however, such a global model is rather difficult to fit, and consequently one

should look for local approximations, depending on the current operating conditions. In such a situation, on-line adaptive control seems to offer an ideal solution.

The algorithm discussed in the previous section can be made adaptive, or self-tuning, by incorporating on-line identification of the parameters. A recursive least squares (RLS) algorithm was implemented in the following form taken from [8]:

$$p(k) = \frac{Q(k-2) \phi(k-1)}{\lambda(k-1) + \phi(k-1)^T Q(k-2) \phi(k-1)} e(k) \quad (7)$$

$$Q(k-1) = \frac{1}{\lambda(k-1)} \left( Q(k-2) - \frac{Q(k-2) \phi(k-1) \phi(k-1)^T Q(k-2)}{\lambda(k-1) + \phi(k-1)^T Q(k-2) \phi(k-1)} \right) \quad (8)$$

$$e(k-1) = y(k) - p^T \phi(k-1) \quad (9)$$

where  $y$  may denote  $\alpha$  or  $q$  and  $p$  may stand for  $p_\alpha$  or  $p_q$ , respectively. The forgetting factor  $\lambda$  was introduced to enable the algorithm to change the estimates of parameters with the change of operating conditions. To avoid the unlimited growth of covariance matrix  $Q$  at the steady state when the input is not persistently exciting the variable forgetting factor policy was implemented:

$$\lambda(k) = 1 - \epsilon \frac{e(k)^2}{\bar{e}(k)^2} \quad (10)$$

where  $e(k)$  is the current prediction error,  $\bar{e}(k)$  is the average prediction error form last 10 samples and  $\epsilon$  is equal to 0.01. As an additional precaution the trace of the covariance matrix  $Q$  was monitored and  $Q$  was reset to diagonal matrix whenever the threshold value was exceeded. Starting values of parameters were taken to be as in (1).

Figure 2 displays the simulation results for a reference model specified as  $1/(z^2-1.8z+0.82)$ . Remarkably exact following of the reference trajectory may be observed, although, surprisingly enough, the performance is slightly worse than in the nonadaptive case. Most probably this is due to the fact that prediction error now changes much more quickly because of the ongoing identification process. Thus, approximating the term  $(y(k+1)-y_{\text{mod}}(k+1))$  by  $(y(k-1)-y_{\text{mod}}(k-1))$  may worsen the

behavior of the system as two values of  $y_{\text{mod}}$  no longer correspond to the same parameter vector. Since the on-line identification process assures (at least in principle) that the prediction error should asymptotically converge to zero it is possible that the correction terms in  $\hat{\alpha}(k)$ ,  $\hat{q}(k)$ , and in control equation (5) ought to be omitted.

The performance of the adaptive nonlinear MAC controller was compared to the linear one, which uses the same control strategy but with a strictly linear model being identified and used for the calculation of the control action. Clear difference between the performance of linear and nonlinear controller can be seen from Figure 3, particularly in control action at the setpoint  $\alpha = 15^\circ$ . The linear identifier has obvious difficulties with fitting the parameters of a linear model to the behavior of the plant which is highly nonlinear in this region. As a result, the control starts oscillating for a while. Also, it was seen that the nonlinear algorithm results in control plots that are more smooth, although they still contain one-pulse spikes. To eliminate these spikes weighting of the increments of control can be introduced into the algorithm with little performance deformation.

#### 4. CONCLUSIONS

The nonlinear control applications to high angle-of-attack aircraft, as reported here, is of a preliminary nature. However, the analysis does suggest that nonlinear adaptive control can be quite effective to stabilize large rapid maneuvers in angle of attack. Of the comparisons made, the on-linear, nonlinear-time-series and adaptation performed the best and was quite superior to a similar linear MAC.

#### 5. ACKNOWLEDGEMENT

The research reported here is supported by NASA Grant No. NAG-1-1081 with supplemental support from NSF Grant No. ECS8913773.

## REFERENCES

- [1] A.D. Modyaev, A.D. Averina, "Analysis and synthesis of discrete control systems based on multidimensional z transforms," in Philosophy of Nonlinear Systems (B. Naumov, ed.), Mir Publishers/CRC Press, 1990.
- [2] K. Harris, "Properties of nonlinear model algorithmic control," Proceedings of 24th Conference on Decision and Control, Ft. Lauderdale, 1985, vol. 1, pp. 663-665.
- [3] H. Stalford, W.T. Baumann, F.E. Garrett, T.L. Herdman, "Accurate modeling of nonlinear systems using Volterra series submodels," Proceedings of the 1987 American Control Conference, Minneapolis, 1987, Vol. 2, pp. 886-891.
- [4] A. Ostroff, "Application of variable-gain output feedback for high-alpha control," AIAA Guidance, Nav. & Control Conf., Boston, 1989.
- [5] A. Ostroff, "Superagility application of a variable-gain output feedback control design methodology," NASA High Angle of Attack Tech. Conf., Hampton, VA, 1990.
- [6] H. Wakamatsu, "Model reference nonlinear adaptive control system using nonlinear autoregressive moving average model derived from Volterra series and its application to control of respiration," Proceedings of IFAC 10th Triennial World Congress, Munich, 1987, Vol. 10, pp. 191-196.
- [7] S.A. Al-Baiyat, "Nonlinear feedback synthesis: a Volterra approach," Ph.D. dissertation, Department of Electrical Engineering, University of Notre Dame, 1986.
- [8] G.C. Goodwin, K.S. Sin, Adaptive Filtering, Prediction and Control, Prentice Hall, 1984.

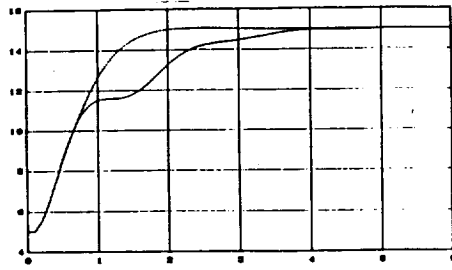


Figure 1a: Step response with non-linear controller vs. nominal response

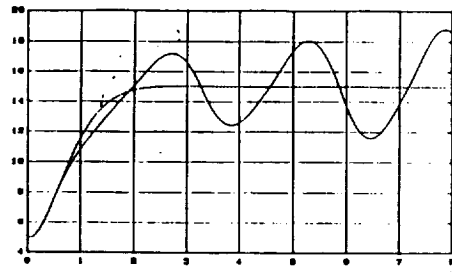


Figure 1b: Step response with linear controller

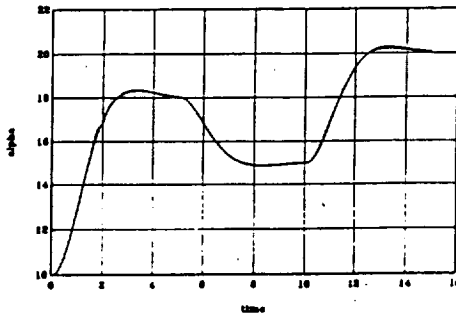


Figure 2a: Nonlinear adaptive MAC (with reference trajectory)

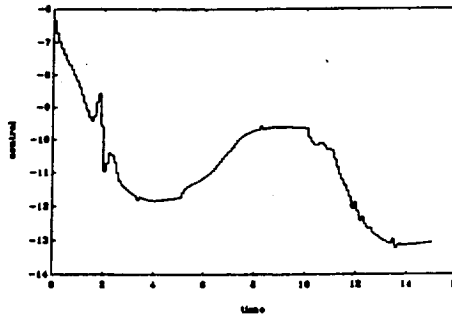


Figure 2b: Nonlinear adaptive MAC

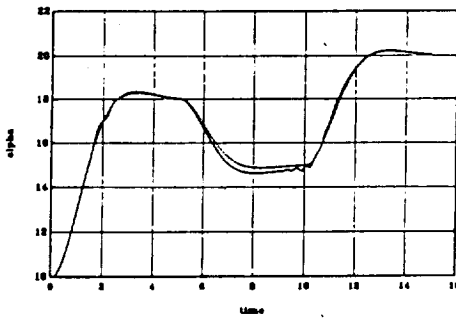


Figure 3a: Linear adaptive MAC (with reference trajectory)

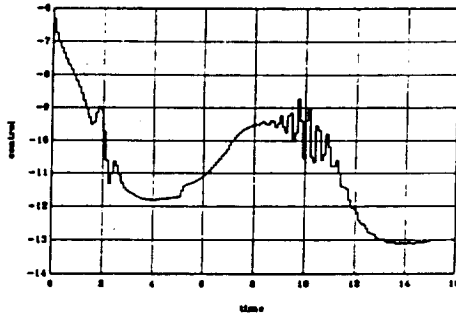


Figure 3b: Linear adaptive MAC

## **APPENDIX C**

### **Analysis of Nonlinear System Stability Using Robust Stability Analysis for Linear Systems**

ANALYSIS OF NONLINEAR SYSTEM STABILITY USING ROBUST STABILITY  
ANALYSIS APPROACH FOR LINEAR SYSTEMS

Jerzy E. Kurek

Instytut Automatyki Przemysłowej, Politechnika Warszawska  
(Inst. of Industrial Automatics, Warsaw University of Technology)  
ul. Chodkiewicza 8, 02-525 Warszawa, Poland  
Fax (22) 29-2962, Tel (22) 49-9616, Tlx 813307 pwpl

During the research author was with  
Department of Electrical and Computer Engineering  
Oregon State University, Corvallis, Oregon 97331-3211, U.S.A.

Summary

The stability analysis of an airplane using its nonlinear model is presented. The analysis is based on the robust stability analysis approach for linear systems. Then, based on analysis, a small static feedback gain is designed such that the robustness of the closed-loop nonlinear system stability is significantly improved.

Acknowledgment

This research was in part supported by NASA Grant No. NAG-1-1081.

## 1. INTRODUCTION

The stability is one of the most important issues in the control system design. Recently there has been observed a great interest in the methodology of robust stability analysis and design of robust control systems for linear dynamic systems [6]. The objective of this paper is to investigate the applicability of this approach for nonlinear dynamic system such as an aircraft flight in high angle of attack/sideslip flight. The unstable control system can result in the plane crash.

There is considered stability of nonlinear, simplified however, model of the airplane. The organization of the paper is as follows. In section 2, the model of the plane is presented. Stability of the aircraft is considered in section 3. Finally, concluding remarks are given.

## 2. THE AIRCRAFT MODEL.

Model of an airplane is highly nonlinear, [4,5]. There are usually, however, used simplified models for control system design, e.g. [1,3,9]. In this paper we consider very simple model given in [8]:

$$\dot{x} = A(x)x + Bu + D \quad (1)$$

where  $x = \begin{bmatrix} \alpha \\ q \end{bmatrix}$  is a state vector,  $\alpha$  is the angle of attack in degrees,  $q$  is the pitch rate in degrees per second and  $u$  is the elevator control in degrees,

$$A = \begin{bmatrix} 9.168c_z(\alpha) & 1 \\ -5.73 & 0 \end{bmatrix}, \quad B = \begin{bmatrix} -1.8336 \\ -8.5950 \end{bmatrix}, \quad D = \begin{bmatrix} -5.473296 \\ 2.865000 \end{bmatrix}$$

and  $c_z(\alpha)$  is a nonlinear function. This function can, however, be approximated as follows:

$$c_z(\alpha) = \begin{cases} -0.072815870 & \text{for } 0^\circ \leq \alpha \leq 14.74^\circ \\ 0.088470922 - 2.3774/\alpha & \text{for } 14.74^\circ < \alpha \leq 17.40^\circ \\ 0.033099050 - 1.4068/\alpha & \text{for } 17.40^\circ < \alpha \leq 18.87^\circ \\ -0.016633734 - 0.4743/\alpha & \text{for } 18.87^\circ < \alpha \leq 28.00^\circ \end{cases} \quad (2)$$

It is easy to find that

$$\begin{aligned} -0.072818087 < c_z(\alpha) \leq -0.048161261 & \quad \text{for } 14.74^\circ < \alpha \leq 17.40^\circ \\ -0.047751524 < c_z(\alpha) \leq -0.041453149 & \quad \text{for } 17.40^\circ < \alpha \leq 18.87^\circ \\ -0.041768869 < c_z(\alpha) \leq -0.033573019 & \quad \text{for } 18.87^\circ < \alpha \leq 28.00^\circ \end{aligned}$$

This model approximates model taken from measured wind tunnel values of the T-2C airplane [7]. It is known that numerical values of  $c_z(\alpha)$  and  $b_2$  are uncertain.

Our purpose is to consider stability of system (1) in the range of angle of attack  $0^\circ \leq \alpha \leq 28^\circ$ , and to find a static feedback which can, eventually, improve the stability of the plane in this range.

### 3. STABILITY ANALYSIS.

Consider linear time-invariant system

$$\dot{x} = Ax \quad (4)$$

where  $x \in \mathbb{R}^n$  is a state vector. Then, assuming that the system is asymptotically stable one can define the following notions, [2].

#### Definition 1.

A connected set  $\Omega_I$  in the system parameters-space (parameters of matrix A) is a robust time invariant stable (RTIS) set for system (4) iff  $A \in \Omega_I$  and every time-invariant system

$$\dot{x} = Ax \quad (5)$$

is asymptotically stable for  $A \in \Omega_I$ .

□

Definition 2.

A connected set  $\Omega_V$  in the system parameters-space is a robust time varying stable (RTVS) set for system (4) iff  $A \in \Omega_V$  and every time-varying system (5) is asymptotically stable for  $A \in \Omega_V$ . □

Then, consider four linear models instead of (2), respectively:

$$c_z(\alpha) = \begin{cases} -0.072815870 & \text{for } 0^\circ \leq \alpha \leq 14.74^\circ \\ -0.048161261 & \text{for } 14.74^\circ < \alpha \leq 17.40^\circ \\ -0.041453149 & \text{for } 17.40^\circ < \alpha \leq 18.87^\circ \\ -0.016633734 & \text{for } 18.87^\circ < \alpha \leq 28.00^\circ \end{cases} \quad (6)$$

It is easy to find that all models are asymptotically stable. We are, however, interested in the set of  $(k_1, k_2)$  such that all the linear closed loop systems will be stable with the following feedback

$$u = Kx, \quad K = [k_1 \quad k_2] \quad (7)$$

An appropriate region  $\Omega_I$  can be easily calculated based on algorithm 2 proposed in [2]. This is, however, only the second order system and one can simply obtain analytical formulas for the RTIS region in this case. The characteristic polynomial for the 2nd order system has the following form

$$s^2 + as + b = 0$$

It is known that all roots of this polynomial are in the left half plane, i.e. a system is asymptotically stable, iff  $a > 0$  and  $b > 0$ . Based on this, the RTIS region  $\Omega_I$  for 'stable' feedback gains was calculated. The region is presented on fig. 1, a dashed line represents RTIS region for model P1,  $0^\circ \leq \alpha \leq 14.74^\circ$ , a dotted model P2 for  $14.74^\circ < \alpha \leq 17.4^\circ$ , a dash-dotted model P3 for  $17.40^\circ < \alpha \leq 18.87^\circ$  and a continuous line model P4 for  $18.87^\circ < \alpha \leq 28^\circ$ . It is easy to see that the system without feedback, i.e.  $k_1 = k_2 = 0$ , sign + on the plane  $(k_1, k_2)$ , is very close to the stability region boundary. One can improve stability assuming appropriate K from  $\Omega_I(k_1, k_2)$ .

Next, RTVS sets  $\Omega_V$  were calculated for these models, according to the algorithm given in [2], for uncertain parameters  $a_{11}$  and  $a_{21}$  in A. They are presented on fig. 2. All four models are inside the RTVS region calculated for the model P4. Moreover, since all time varying (nonlinear)  $a_{11}=9.168c_z(\alpha)$  is smaller than nominal values used in linear models it means that the whole nonlinear system (1) is asymptotically stable for  $0^\circ \leq \alpha \leq 28^\circ$ . However, there is a very small upper bound for  $a_{11}$  in this model, namely

$$+\Delta a_{11} < 0.0227$$

This can cause that with small system uncertainty the system can be unstable. The vertexes of RTVS quadrilateral  $\Omega_V$  on the plane  $(\Delta a_{11}, \Delta a_{21})$  are as follows:

$$V_{V0} = \{ (-176.5, 0), (0.0226, 0), (0, -0.2274), (0, 0.2944) \}$$

In order to improve system stability feedback gain matrix K was chosen from  $\Omega_I$ . Intuitively, it seems that a good gain is a small one - a high gain can result in a lack of system controllability because of saturation of the control input, and such that the stability margin with respect to K will be rather large.

Thus, the good choice seems to be  $K_1 = [0 \ 0.2]$ . For this gain one obtains significant improvement of RTVS set. This set is shown on fig. 3. In this case also all models are inside the  $\Omega_{I1}$  calculated for the model P4. However, an upper bound for  $a_{11}$  is more than 8 times greater:

$$+\Delta a_{11} < 0.1835$$

Also range for uncertain parameter  $a_{21}$  is almost 6 times larger. Indeed, the vertexes of RTVS quadrilateral in this case on the plane  $(\Delta a_{11}, \Delta a_{21})$  are as follows

$$V_{V1} = \{ (-25049, 0), (0.1835, 0), (0, -3.547), (0, 3.211) \}$$

Then, it was considered feedback gain  $K_2=[0.2 \ 0]$ . This gain, however, seems to be worse situated in the RTIS set  $\Omega_I$  than  $K_1$  considering the stability region with respect to  $K$ . Nevertheless, also in this case one obtains improvement of robust stability for the closed loop system. The appropriate RTVS set  $\Omega_V$  is shown on fig. 4. In this case an upper bound for  $a_{11}$  is as follows

$$+\Delta a_{11} < 0.0613$$

Similarly, range for perturbation in  $a_{21}$  is larger than for  $K=0$ . The vertexes of RTVS set  $\Omega_{V2}$  are as follows

$$V_{V2} = \{ (-65.15,0), (0.0613,0), (0,-0.5770), (0,1.3641) \}$$

It should be noted that all RTVS sets were calculated under assumption  $Q=I$  in algorithm 3 [2].

From the above analysis follows that relatively small static linear feedback gain  $K=[0 \ 0.2]$  significantly improves stability of the system. It should be emphasized that every nonlinear/time-varying system (1) with  $a_{11}$  and  $a_{21}$  from the obtained RTVS set  $\Omega_{V2}$  will be asymptotically stable. This way we have designed a robust-stable nonlinear closed-loop system.

#### 4. CONCLUDING REMARKS.

A robust-stable nonlinear controlsystem has been designed. It is shown that small linear static feedback gain can significantly improve stability of the airplane. The feedback gain seems to be so small that it should not constrain control signal during plane maneuvering. This should also results in better a controllability of the plane.

The stability analysis and feedback gain synthesis were done using methods designed for linear systems [2]. This, approach can be also used for more complicated nonlinear systems. For instance,

assuming as a base model for the airplane, the linear 9th order model given in [1,9]. This model is unstable, but, as it was shown in [2], one can deal also with unstable models using the same approach.

Presented results also show the power of the approach proposed in [2].

#### REFERENCES.

- [ 1] S.Grag, D.L.Mattern and R.E.Bullard, "Integrated flight/propulsion control system design on a centralized approach", J. Guidance Control and Dynamics, vol. 14, 1991.
- [ 2] J.E.Kurek, "Robust stability region for linear systems - part I: continuous-time systems", IEEE Trans. Automat. Control, submitted.
- [ 3] R.R.Mohler et. al., Nonlinear stability and control study of highly maneuverable high performance aircraft, OSU-ECE report NASA 91-01, Oregon State University, 1991.
- [ 4] R.R.Mohler, Nonlinear systems v. 1: Dynamics and control, Prentice-Hall, Englewood Cliffs, 1991.
- [ 5] A.J.Ostroff, "Application of variable-gain output feedback for high-alpha control", AIAA Guidance Navigation and Control Conf., Boston, paper No. 89-3576, 1989.
- [ 6] D.D.Siljak, "Parameter space methods for robust control design: a guided tour", IEEE Trans. Automat. Control, vol. AC-34, pp. 674-688, 1989.
- [ 7] H.Stalford, "Application of the estimation-before-modeling (EBM) system identification method to the high angle of attack/sideslip flight of the T-2C jet trainer aircraft", Naval Air development Center Report NADC-76097-30, vol. III, 1979.
- [ 8] H.Stalford, W.T.Baumann, F.E.Garret, T.L.Herdman, "Accurate modeling of nonlinear systems using Volterra series submodels", Proc. 1987 American Control Conference, Minneapolis, vol. 2, pp. 886-891, 1987.
- [ 9] T.Troutet, S.Garg, W.C.Merrill, "Neural network application to aircraft control system design", Proc. AIAA Guidance, Navigation and Control Conference, New Orleans, Louisiana, vol. 3, pp. 993-1009, 1991.

Fig. 1. The RTIS region on plane  $(k_1, k_2)$  for P1, P2, P3, P4

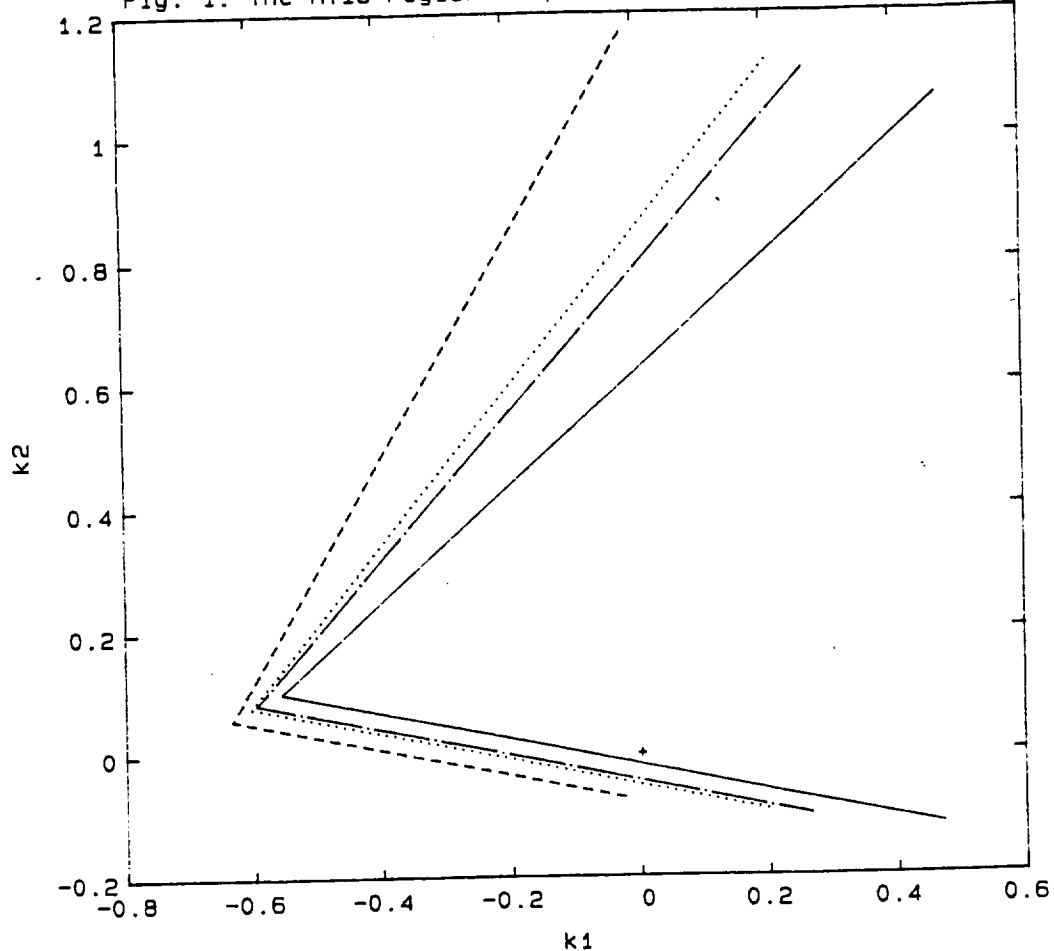


Fig. 2. The RTVS region for P1, P2, P3, P4 with  $K=[0, 0]$

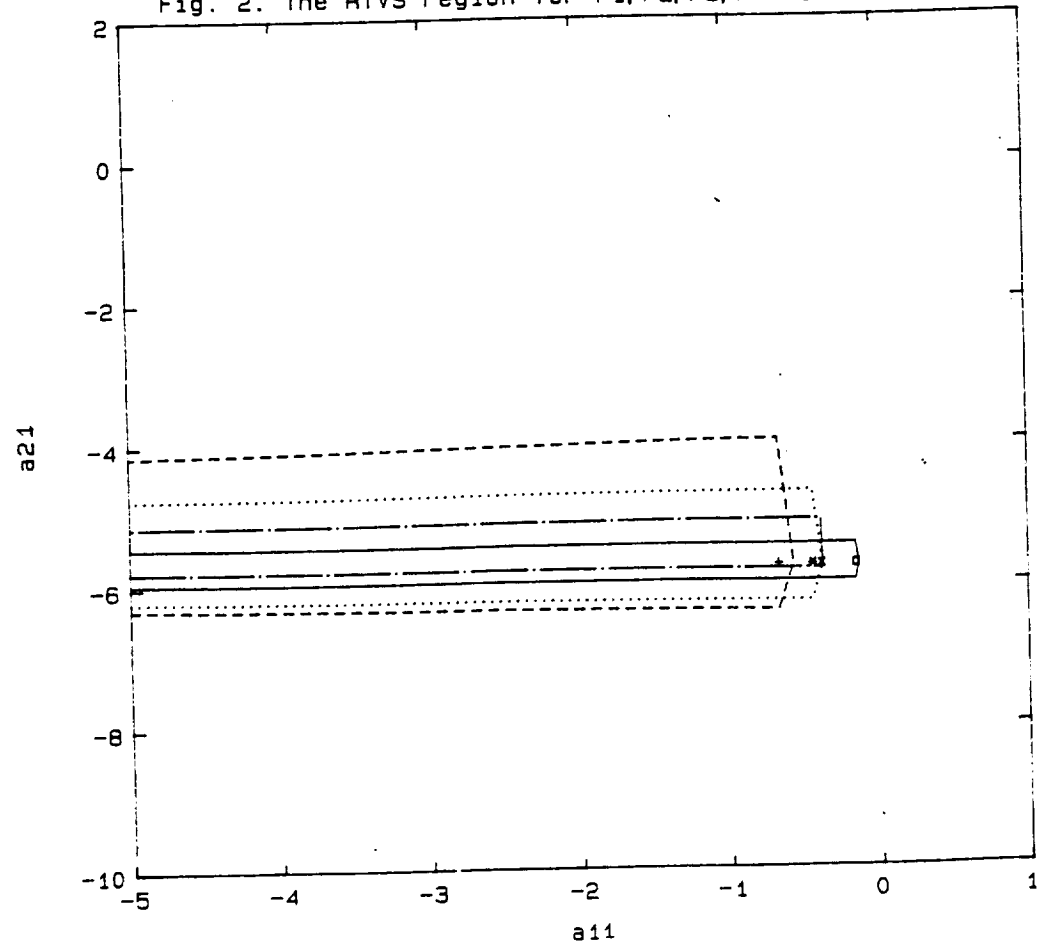


Fig. 3. The RTVS region for P1, P2, P3, P4 with  $K=[0, 0.2]$

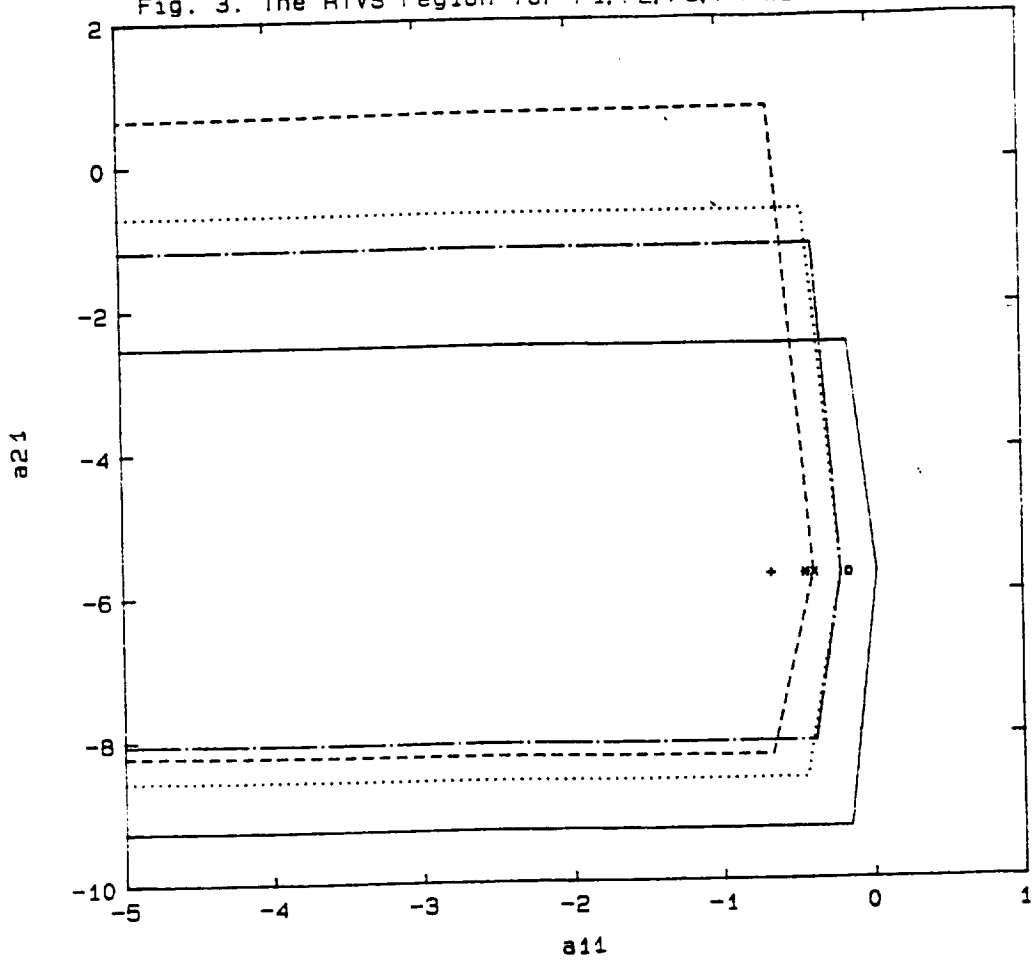


Fig. 4. The RTVS region for P1, P2, P3, P4 with  $K=[0.2, 0]$

